Sea Clutter Simulation

Titus Oluwale Oyedokun

A dissertation submitted to the Department of Electrical Engineering,
University of Cape Town, in partial fulfilment of the requirements
for the degree of Master of Science in Engineering.

Cape Town, May 2012

Declaration

I declare that this dissertation is my own, unaided work. It is being submitted for the degree of Master of Science in Engineering in the University of Cape Town. It has not been submitted before for any degree or examination in any other university.

Signature of Author .....

Cape Town

14 May 2012

Abstract

This dissertation presents the results of a study, the aim of which was the prediction of sea clutter characteristics including the temporal properties of the return signals as observed by a maritime surveillance radar system.

The compound K distribution model used to generate clutter amplitude statistic enables the simulation of sea clutter with a good level of approximation to real radar data and this model forms the basis for the simulation of sea clutter amplitude statistic in this dissertation.

Using this distribution, a sea clutter simulator is designed to generate correlated K distributed random variates from a predefined correlation function using the method by Ward and Tough[1]. Results from the sea clutter simulator shows that the simulated correlated random variates fits the theoretical K distribution PDF.

Experimental sea clutter measurements were carried out using an experimental netted radar system. This was done at Scarborough Cape Town. Result obtained from the monostatic node is presented. This shows the amplitude statistics of the clutter as well as the temporal variation of the Doppler spectrum. Conclusions are drawn based on this results and suggestions made for further work.

To my family,

for all their support and guidance.

Acknowledgements

I would like to thank the following parties for their assistance and involvement in the completion of this project:

- My supervisor Prof Michael Inggs for his advice and guidance throughout this dissertation.
- Fellow colleagues at the Radar remote sensing group at the University of Cape Town for their various contribution towards the completion of this dissertation.
- I would also like to thank member of the Sensors, Systems and Circuits research group at the department Electronic & Electrical Engineering, University College London mostly Waddah Al-Ashwal and Matthew Ritchie for their assistance with the analysis of NetRad data and their various contributions to the project.
- I would also like to thank Prof Simon Watts for his invaluable inputs.
- I would like to thank Dr Glen Davidson for making available his sea clutter simulation toolbox and for all assistance offered.
- I would also like to thank Dr Robert Tough for his helping to explain sea clutter simulation concept during the Advance radar mathematics course offered at UCT 2011.
- My appreciation goes to my family for the love and support they have shown to me throughout the years.

Contents

List of Figures

List of Tables

List of Symbols

$\Gamma(.)$	—	Gamma function
θ_{az}	—	antenna azimuth beamwidth
c	—	Speed of light
θ_{sw}	—	direction of sea swell
θ_g	—	grazing angle
λ	—	radar wavelength
v	—	shape parameter of gamma and K distribution
b	—	scale parameter of the gamma and K distribution
ρ	—	range resolution
σ	—	radar cross section (RCS)
τ	—	pulse length
A	—	area of scattering surface
K_v	—	modified Bessel function of the second kind
p_c	—	mean clutter power
x	—	mean local clutter intensity
σ^0	—	Clutter reflectivity
β	—	Weibull scale parameter
α	—	Weibull shape parameter
G	—	Antenna gain
L	—	propagation loss and other losses
$erfc$	—	the error function

Nomenclature

Azimuth—Angle in a horizontal plane, relative to a fixed reference, usually north or the longitudinal reference axis of the aircraft or satellite.

Beamwidth—The angular width of a slice through the mainlobe of the radiation pattern of an antenna in the horizontal, vertical or other plane.

Doppler frequency—A shift in the radio frequency of the return from a target or other object as a result of the object's radial motion relative to the radar.

PRF—Pulse repetition frequency.

Range—The radial distance from a radar to a target.

FFT—Fast Fourier transform

UCT—University of Cape Town

UCL—University College London

CDF—Commutative density function

NetRad—Netted radar system

RCS—Radar cross section

PDF—Probability density function

ACF—Autocorrelation function

MNLT—Memoryless non-linear transform

Chapter 1

Introduction

1.1 Background

Sea clutter are backscatter returns from a patch of the sea surface when illuminated by a radar pulse. This is as a result of a complex interaction between incident electromagnetic waves and the sea surface. This backscatter often interferes with the intended received signal as huge sea spikes increases the rate of false alarm and depending on the detection threshold, it can lead to missed detection [2].

There are several applications of the study of sea clutter. Apart from maritime surveillance, progress has been made recently in the area of remote sensing of which the sea is an important component [6]. For example, space-based radars are used for oceanography. In this application, the return backscatter off the sea surface are wanted and aids the prediction of wave patterns on the ocean, wave height, and the direction and speed of the wind amongst others [2].

However, for maritime surveillance applications, accounting for the clutter in the detection process remains a key requirement for maritime radars [7]. For surface or airborne radars operating in a maritime environment, this return is unwanted. Examples of such radar systems include: maritime surveillance radar fitted on planes, radars fitted on Navy ships, coastal surveillance radar mounted along the coastal line amongst others [2]. These radars have many operating modes, but in particular they are used for long-range surveillance of surface ships and the detection and identification of small targets [2]. Targets of this nature can be small boats on the sea such as used in poaching and submarine masts.

In all cases, the radar designer must understand the characteristics of the backscatter from the sea in order to either relate the signal to the ocean characteristics or to achieve the performance required by the radar users. These characteristics are found to vary according to the radar parameters, the viewing geometry and weather conditions [6, 2]. With a good knowledge of the nature and behaviour of the clutter, appropriate signal processing techniques can be applied within the radar to detect targets immersed in clutter.

When sea clutter is measured over a relatively short time interval of about a second, the sea clutter returns shows a negative exponential distribution often referred to as Gaussian speckle. This clutter returns decorrelates completely within the interval of observation. However, as the observation time increases, the statistics of the observed clutter varies from that of just the Gaussian shape but can now be approximated by the gamma distribution. Thus the Gaussian speckle and its gamma distributed randomly varying local power are brought together in the compound K model of sea clutter. The correlation properties of the more slowly varying gamma component of the clutter are the one that affects the radar performance. Thus the need of the compound representation of the clutter processes [1].

Researchers in this field [2] have developed statistical models and simulation techniques to aid the simulation of targets embedded in clutter, to evaluated signal and image processing concepts to minimise the effect of clutter.

In addition, to aid with formula based estimates of the effect of clutter, through parameters. These models are used to simulate the amplitude statistics of clutter and also to investigate the temporal characteristic of sea clutter for various conditions.

The radar remote sensing research group at University of Cape Town (UCT) has taken interest in this area of radar research and aims at a later stage, to include this simulator into an existing muiltistatic radar simulator developed by Brooker [8].

1.2 Objectives

The main objective of this dissertation is to design a sea clutter simulator. This is a random number generator that generates clutter whose probability density function (PDF) matches the desired K distribution PDF. This will take in radar parameters, the viewing geometry and weather conditions to determine the amplitude statistic of sea clutter. Perform statistical goodness of fit tests on the outcome of the simulator to determine the accuracy of the random number generator.

In addition to this, the project seeks to investigate the coherent nature of sea clutter and methods used to characterise the temporal variation of the Doppler spectrum as observed from a single range cell. The project also endeavours to show an analysis of real sea clutter data measurements taken from an S band netted radar system (NetRad) by comparing the amplitude statistics of the sea clutter to the K distribution PDF and calculate the Doppler spectrum to show the temporal variation of sea clutter as observed by the radar. Finally, the study aims to draw conclusions on the performance of the simulator and give recommendations on how the simulator might be improved with possible future work.

1.3 Classical modelling approach to sea clutter simulation

Sea clutter modelling to date for radar design and development, particularly at low grazing angles, has been empirical [6]. This is done by analysing measured sea clutter data to be able to model features of sea clutter. Another alternative to this is by using a description of the sea surface and Electromagnetic (EM) scattering calculations. Although this method seems to be ideal, the complexity of the EM scattering mechanisms and the characterisation of the sea surface are not that simple. However, the difficulties of empirical characterisation in complex oceanographic and littoral environments are leading to increasing emphasises on the physical approach [6].

It has been found that when measuring sea clutter, the probability of relatively large signal occurrence is higher than that predicted from a Rayleigh distribution model. Such distributions are said to have "long tails" [9, 10, 11, 6]. The "long tail" of the distribution is crucial in setting target detection threshold in order to minimise both false alarms and missed detections [2]. As a result, other non Gaussian statistical distributions other than the Rayleigh model have been explored to characterise sea clutter returns. These include the Weibull, K and log normal distributions [6, 12, 13].

The K distribution, however, is the most widely used model in the study of sea clutter. [2, 6, 11, 10, 9, 14]. This is because of its compound form that handles the correlation features as well as the clutter amplitude statistics. The K distribution is defined by the shape parameter and scale parameter. The former defines the spikiness of sea clutter, while the latter accounts for the power characteristics of the echo signal [2].

There are several contributing factors to the varying amplitude characteristic of sea clutter. The wind speed plays a major role as it determines the shape and roughness of the sea surface. Other factors that influence the accurate modeling of sea clutter include: the radar and viewing geometry parameters [9, 2]. Combined with a good statistical model, the knowledge of these parameters allows for an effective prediction of the amplitude characteristics of sea clutter.

Another aspect in simulating sea clutter is to understand the temporal characteristic of the clutter. Coherent radars employing Doppler processing can distinguish targets from clutter if the target's radial velocity is sufficiently high [2]. However, some targets of interest will have Doppler shifts that are not significantly different from the Doppler spectrum of the sea clutter. In these cases, it is important for the radar designer to have a detailed understanding of the characteristics of the Doppler spectrum for all the different conditions likely to be encountered. Different methods have recently been proposed to be able to regenerate the Doppler spectrum evolving over time by Watts [15] and Davidson [10] amongst others. This research exploits these modelling techniques to the simulation of sea clutter amplitude statistic as well as the Doppler spectra of sea clutter.

1.4 Dissertation outline

Chapter 2 presents a literature review on areas of sea clutter modelling pertaining to this dissertation. The characteristics of sea clutter are known to vary according to the radar parameters, the viewing geometry and weather conditions. The statistics of these variation are usually described using PDFs. This stochastic approach is reviewed. The coherent characteristics of sea clutter and the temporal variation of the clutter are briefly disused in this chapter reviewing some recent results obtained by other researchers who have worked on this.

Chapter 3 is divided into two sections. The first section presents a method by Ward and Tough [1] that is used to generate correlated K distributed random numbers with specified correlation function. This method is used to model the amplitude statistics of sea clutter. The second section presents a recently developed method by Watts [15] for the simulation of coherent sea clutter . The method characterises the temporal variations of the Doppler spectrum observed from a single range cell. The derivation of this method is explained in this section with the implementation and comparison with an S band experimental radar data set presented in Chapter 5.

Chapter 4 presents the implementation of a sea clutter simulator procedure for the amplitude statistic of sea clutter. It is divided into two main sections. The first section presents a description of the software package for the synthetic generation of sea clutter return that is based on the methodology given in Chapter 3 section 1. The second section presents the validation of the amplitude statistic result.

Results obtained from the run of the simulator shows that for small values of the shape parameter, the peak values increases relative to the mean. This is in accordance with literature. The validation of the generation of synthetic sea clutter returns was done by computing the Kolmogoroff-Smirnoff (K-S) statistic goodness of fit test. Results obtained shows that indeed the simulated clutter arises from the K distribution. The simulated correlated K distribution random variate was also fitted to the theoretical K distribution and there shows a good match.

Chapter 5 deals with experimental measurements of sea clutter. Observing both the amplitude distribution of the clutter as well as the temporal variation of the Doppler spectrum. The S-band (NetRad [4]) data set was analysed to show some of the temporal behaviour of sea clutter and to establish some features that the simulator aims to reproduce. To check that the radar data fits the well known K distribution statistical model, samples from a single range cell was fitted to the K distribution. The amplitude PDF of the clutter fits the K distribution for the VV polarisation. This implies that for the monostatic recordings of NetRad, the clutter as observed can be well modelled by the K distribution.

The Doppler spectra from a single range gate were calculated. This shows the variation of the clutter from a single range cell for the duration of observation. It can be observed that the clutter intensity varies with time. Also the spectrum appears asymmetric in shape with some Doppler excursions

which might have been as a result of wind gust.

Chapter 6 draws conclusions and suggest further work. The major findings resulting from this work is that the generated clutter indeed arises from the K distribution which is best known to model sea clutter amplitude statistic of which the K-S test carried out proves. From the sea clutter experiment carried out using the NetRad system, plots of the Doppler spectrum shows the temporal behaviour of the sea.

Chapter 2

Characteristics of Radar Sea Clutter

2.1 Overview

Radar operating in maritime environment will inevitably encounter backscatter off the sea surface which is often referred to as sea clutter. In remote sensing system applications, the reception of this backscatter forms the main purpose of the radar **[2]**. For example space-borne synthetic aperture radars used for oceanographic studies, gather data on waves and currents. Scatterometers measures average backscatter over a large distance to predict the wind speed and direction over the sea surface.

For other applications such as airborne radars operating over the sea, radars used for surveillance, or to detect submarine periscope, backscatter from the sea is unwanted and may interfere with the radar's operation. The characteristic of sea clutter over this range of applications vary widely. The radar designer has to develop suitable signal processing techniques to predict performance under different conditions. Additionally, this is achieved by having a good understanding of the clutter characteristics and behaviour under these conditions. An important step in simulating sea clutter is to develop accurate statistical models for the clutter. These models should be able to somewhat reproduce the amplitude and temporal characteristic of sea clutter under different environmental conditions. Of recent there have been increased interest in not only monostatic sea clutter but also bistatic sea clutter [16]. But the main focus of this literature review will be on monostatic sea clutter.

In this chapter, features used to characterise sea clutter returns will be discussed. This includes the different statistical models that can be used to model sea clutter. In particular attention is paid to the compound K distribution model which is well known to replicate sea clutter more accurately than other non-Gaussian statistical models.

2.2 The sea surface

Observation of radar sea clutter are usually associated with particular characteristics of the sea surface and the environment such as sea waves as a result of the wind speed [2]. It can be seen from the observation of the sea surface as shown in Figures 2.1 and 2.2. that it is not a random rough surface but contains significant structure. When the wind blows it generates small ripples, which grow and transfer their energy to longer waves. At some point the waves become large enough to break and this redistributes the wave energy further. All of these waves and the breaking events are reflected in the temporal and spatial variation of clutter returns and the nature of such variation needs to be characterised [17, 2].

Figure 2.1: Wave breaking on the sea surface (courtesy of NetRad trials, Scarborough Cape Town)

Figure 2.2: The sea surface before the onset of significant wave braking (courtesy of NetRad trials, Scarborough Cape Town)

The following are some definition of terminologies that are used to describe the sea surface and the environment. The definitions are given in [2, 5, 9]:

Wind wave: As a result of the action of the wind on the water surface. a swell remains when the wind stops blowing.

Capillary wave: A wave whose velocity of propagation is controlled primarily by the surface tension of the liquid in which the wave is travelling.

Gravity wave: A wave whose velocity of propagation is controlled primarily by gravity. Waves of length grater than 5cm are considered gravity waves.

Fetch: Is a distance of the sea surface over which seas are generated by a wind having a constant direction and speed.

Duration: The length of time the wind blows.

Sea state: The numerical or written description of ocean-surface roughness. This can be defined in terms of the significant wave height, $h_{1/3}$ which is the average height of the highest one third of the waves. There are tables that describe this sea state. The Douglas sea state table [5] shown in Table 2.1 is one of the them. In this dissertation, this table will be used to estimate the sea state for simulation purposes.

Table 2.1: The Douglas sea state table [5]

Douglas sea state	Description	Wave height h1/3(ft)	Wind speed (kn)	Fetch(nmi)	Duration (h)
1	Smooth	0-1	0-6		
2	Slight	1-3	6-12	50	5
3	Moderate	3-5	12-15	120	20
4	Rough	5-8	15-20	150	23
5	Very rough	8-12	20-25	200	25
6	High	12-20	25-30	300	27
7	Very high	20-40	30-50	500	30
8	Precipitous	>40	>50	700	35

The sea state is an important parameter in determining the clutter reflectivity σ^o. There are many theoretical models for the clutter reflectivity based on different description of the roughness of the sea surface. These models, which are discussed in Section 2.4.4 are mainly based on empirical measurements and observations. They provide a good estimate of the range of values of σ_0 likely to be encountered in different conditions [2].

2.3 Radar equation and sea surface geometry

The type of radar used and its specifications contributes to the observed clutter characteristics. Important radar parameters includes the radar carrier frequency, the bandwidth, antenna beam-width, pulse repetition frequency, transmitted power, receive and transmit polarisations. The knowledge of these parameters allows for the prediction of sea clutter amplitude statistic.

A monostatic radar with a common transmitting and receiving antenna, the clutter power at the output of the radar receivers matched filter is given by:

$$p_c = \frac{p_t G^2 \lambda^2 \sigma^o . A_c}{(4\pi)^3 R^4 L} \tag{2.1}$$

Where

p_t is the transmit power
G is the antenna gain
σ_o is the normalised radar cross section
A_c is the area of sea illuminated
R represent the range
L represent all Losses

In equation (2.1), A_c is as a result of the viewing geometry. This is the cross section area illuminated by the radar pulse. This will change as the viewing geometry changes that is, for different elevation angles and azimuth beamwidths. This is defined in Equation 2.2

$$A_c = \alpha \rho R \theta_{az} \sec(\theta_g) \tag{2.2}$$

where
θ_{az} is the antenna beam-width
θ_g is the grazing angle
ρ is the range resolution $\rho = c/2B$
α accounts for the actual compressed pulse shape and the azimuth beam shape

As shown in Figure 2.3, the area of the clutter patch is defined by the azimuth beam-width and the pulse length. h represent the vertical height of the radar off the base line. Coastal land based radar are usually place on a cliff or areas around the coast line to give the required grazing angle.

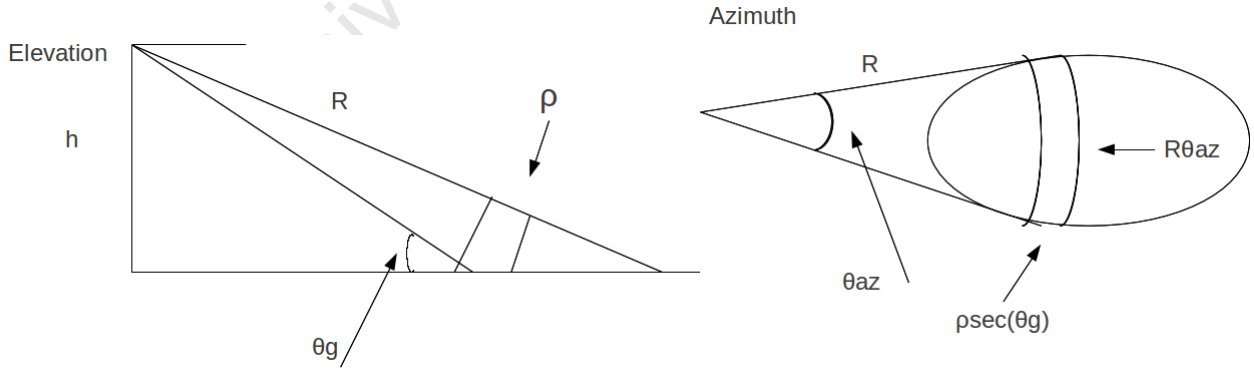

Figure 2.3: Clutter illuminated patch size [2]

For sea clutter, it is expected that the clutter will fluctuates about this mean value σ_0 for the period of observation. Stochastic approach has mainly been used in literature to characterise these returns in the form of probability distributions. This forms the basis of generating large surrogate data to represent actual data as observed by a radar. Subsequent sections will aim to explain the different statistical models as found in literature and how they can be used to simulate sea clutter.

2.4 Amplitude characteristics of sea clutter

In the last 30 years, researchers working in this field have approach the study of sea clutter mainly from an statistical stand point [6]. As physical approach using a description of the sea surface and EM scattering calculation might seen as ideal, the EM scattering mechanism and the characterisation of the sea surface is complex [6]. Thus, sea clutter modelling to date for radar design and development have been by use of empirical models [2, 10, 6].

Ward et al.[2] and others who have worked on deriving appropriate models for sea clutter has highlighted the usefulness of the compound representation of the clutter process. The mean reflectivity represents the mean clutter power. The instantaneous power received from a single radar resolution cell varies about this mean clutter reflectivity. This variation is characterised by the PDF of the returns. In [2] contributions to the fluctuation has been identified as when the wind blows and as such roughens the sea surface, Bragg scattering occurs which form ripples with spacing of half a wavelength. The wind waves and swell then cause the surface slope to change, thus resulting in a modulation of the local backscatter intensity.

At low radar resolution, and for large grazing angles clutter amplitude fits the Rayleigh distribution model. However, as the radar resolution increases, and for smaller grazing angles, the clutter characteristics is known to departs from that of the Rayleigh model [2]. The probability of relatively large signal occurrence is higher than that predicted by a Rayleigh model and the return are often described as 'spiky'. The PDF of the amplitude clutter return is said to exhibit long tails. The "long tail" of the distribution is crucial in setting target detection threshold in order to minimize both false alarms and missed detection. As a result, other statistical distributions have been explored to characterise the clutter return. These includes the Weibull, log-normal and K-distributions [12, 13, 2]. In particular the K distribution has been shown to model the "long tails" more effectively because of its compound formulation [2].

2.4.1 The choice of sea clutter amplitude distribution

The choice of the amplitude distribution used in modelling sea clutter are driven by the fact that there is a need to take into account both the amplitude and temporal behaviour of the clutter. The magnitude of the sea clutter changes as a result of the wave height which is due to the wind speed. For an accurate representation of sea clutter for simulation and data analysis, the statistical model to be used must incorporate this dynamic behaviour of sea clutter. Table 2.2 presents the probability distribution function of some well known non-Gaussian statistical distributions and their moments.

Table 2.2: Probability density functions of Non-Gaussian distribution models

Distribution models	PDF	Moments
Weibull	$p(z) = \beta \frac{z^{\beta-1}}{\alpha^{\beta}} e^{-(z/\alpha)^{\beta}},\ z \geq 0$	$< z^n >= \alpha^n \Gamma(n/\beta + 1)$
Log-Normal	$P(z) = \frac{1}{z\sqrt{2\pi\sigma^2}} \exp\left(-\frac{(\log[z]-m)^2}{2\sigma^2}\right);\quad z \geq 0$	$< z^n >= \exp(nm + n^2\sigma^2/2)$
K distribution	$P(z) = \int dx P(z\|x) P_c(x) = \frac{2b^{(v+1)/2} z^{(v-1)/2}}{\Gamma(v)} K_{v-1}(2\sqrt{bz})$	$< z^n >= \frac{b^{-n} n! \Gamma(v+n)}{\Gamma(v)}$

The Weibull distribution is characterised by the scale parameter α and the shape parameter β , σ and m are the standard deviation and the mean for log-Normal distribution respectively. v and b are the shape parameter and the scale parameter for the K distribution respectively.

From a review of literature [18, 9, 19, 2**?**], the following can be concluded;

The statistics of sea clutter at large grazing angles and low radar resolution, follows the Rayleigh distribution model. however, as the radar resolution increases, and for smaller grazing angles, the clutter characteristics is known to depart from that of the Rayleigh model. The probability of relatively large signal occurrence is higher than that predicted by a Rayleigh model and the return are often described as 'spiky'. The PDF of the amplitude clutter return is said to exhibit long tails. The long tail of the distribution is crucial in setting target detection threshold in order to minimize both false alarms and missed detection.

From many statistical analyses of radar sea clutter, it has been proven that the K distribution can serve as a limiting distribution for sea clutter. Thus making the K distribution the most appropriate model for sea clutter especially in the low probability of false Alarm region.

Non-Gaussian statistical distribution such as mentioned in Table 2.2 used for sea clutter, unlike the K distribution are not derived from a physical model or clutter scattering mechanism. The choice and validation are mostly based on their agreement with experimental data. Although these models of sea clutter can fit the amplitude statistics, they do not describe the temporal and spatial correlation in the data.

Figure 2.4,2.5 and 2.6 shows the PDF and amplitude plots of these different distributions. The time series data was generated from the Weibull PDF. Implementing the mathematical description of the probability density function in Matlab code, Weibull random clutter was generated. The Weibull shape parameter and scale parameter was varied to give the Figure 2.4. Likewise in Figure 2.5 the lognormal PDF was plotted for different mean and variance. Figure 2.6 shows the K distribution PDF also ploted for various shape and scale parameters. In each case, the time-series data was generated using the inbuilt random number generator functions in Matlab.

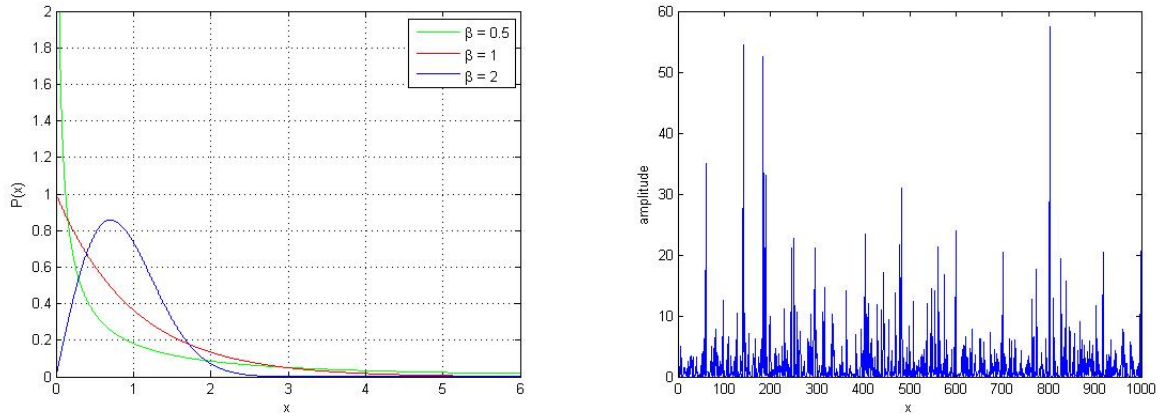

Figure 2.4: Weibull probability density functions for various shape parameter and scale parameter =1. b) shows the Weibull noise with $\alpha = 1$, $\beta = 0.5$

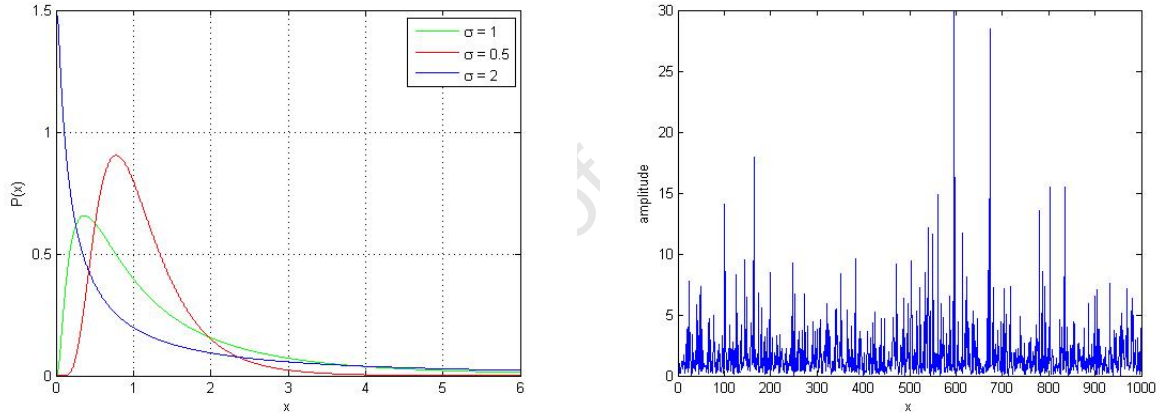

Figure 2.5: Log-normal probability density functions with m = 0 and the Lognormal distribution noise for m = 0 and $\sigma = 1$

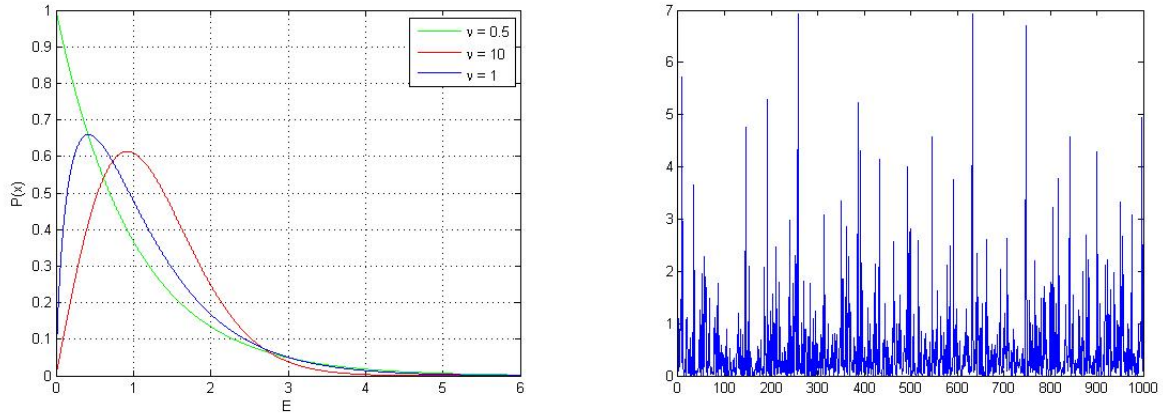

Figure 2.6: K probability density function for scale parameter set to 1 and different shape parameter. Also shown is K distributed random variate for 0.5

An example of fitting PDF to real radar sea clutter data is shown in Figure 2.7. The data set used in this plot is taken from Farina et al [3]. The data from a single range cell. By visual inspection it can be noticed that the amplitude distribution of the data best fit the K distribution although there is also a good fit to the Weibull distribution. Also, in Ward et al. [2]; Farina et al [20], the K distribution has been tested on several other data set and has proven to be the distribution function of choice.

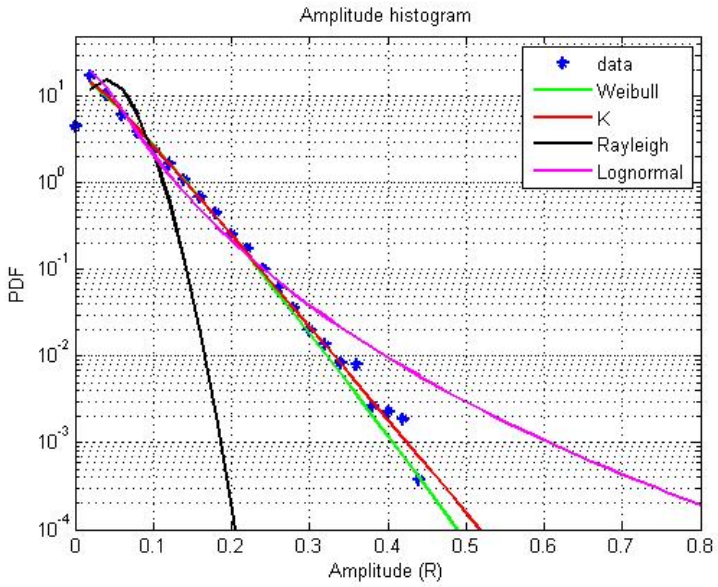

Figure 2.7: Fitting Non-Gaussain statistical distribution to real radar data Farina et al [3]

An extensive comparison between these distributions can be found in Dong [21]. The K distribution thus provides a good description of the clutter amplitude statistic and has an advantage in handling the coherent nature of sea clutter.

2.4.2 The K-distribution clutter model

The K distribution as it has been developed by the observation of real clutter data over a wide range of conditions can be modelled mainly by two components [22, 2] the local power and the speckle component.

The local power x which is the slowly varying component can be associated with the large scale structure of the sea. It has a long temporal decorrelation period of the order of seconds. The Gamma distribution has shown to provide best fit to this observation and thus modelling the local power x by

$$P_c(x) = \frac{b^v}{\Gamma(v)} x^{v-1} \exp(-bx) \tag{2.3}$$

This distribution is characterised by a scale parameter, b, and a shape parameter, v, which depends on sea conditions and the radar parameters.

The second component, termed the "speckle" component, is a fast varying component identified with the changing interference between capillary wave scatterers. The speckle component has a shorter decorrelation time than the local power in the order of milliseconds. This is modelled by an exponential distribution PDF of intensity z with mean x

$$P(z|x) = \frac{1}{x}\exp(-\frac{z}{x}) \tag{2.4}$$

Integration on x gives the K distribution PDF

$$P(z) = \int dx P(z|x)P_c(x) = \frac{2b^{(v+1)/2}z^{(v-1)/2}}{\Gamma(v)}K_{v-1}(2\sqrt{bz}) \tag{2.5}$$

where $K_{v-1}(2\sqrt{bz})$ is the modified Bessel function of the second kind. $\Gamma(v)$ is the Gamma function and b is the scale parameter and v is the shape parameter.

The moments are given as

$$< z^n >= \frac{b^{-n}n!\Gamma(v+n)}{\Gamma(v)} \tag{2.6}$$

Figure 2.6 shows plot of the K distribution PDF from Equation 2.5 for various values of shape parameter, v, and with the scale parameter set to unity. Typical values of v are in the range of 0.1 $\leq v \leq \infty$. When $v = \infty$ the K distribution reduces to the Rayleigh distribution, while for small values of $v < 1$, the spikiness of the clutter increases [2].

2.4.3 Empirical models for the prediction of the shape parameter

The shape parameter v can be obtained by using an empirical model. The model depends on the radar, geometric parameters and the sea conditions [2]. This model which was developed through the analysis of experimental data at I-band (9-10 GHz) and also known to work well from 5 to 35 GHz [23], explains the dependence of the shape parameter on radar, environmental and geometric environment and can be generally applied in the simulation of sea clutter [24, 2, 9, 25]. This is given by:

$$log_{10}v = \frac{2}{3}log_{10}(\theta_g) + \frac{5}{8}log_{10}(A_c) - K_{pol} - \frac{\cos(2\theta_{sw})}{3} \tag{2.7}$$

where;

θ_g	Grazing angle in degrees
A_c	Radar resolved area
k_{pol}	Polarisation dependent parameter (1.39 for VV and 2.09 for HH)
θ_{sw}	Aspect angle with respect to the swell direction

The scale parameter b represents for the power characteristics of the returned signal. The smaller the value of b the more powerful the reflected signal is from the sea surface and this can be predicted from the knowledge of the mean clutter reflectivity and the radar parameters. For a patch of sea of area, A, illuminated by a radar pulse, the radar mean cross-section (RCS) is given by $\sigma_A = \sigma_o.A$, where σ_0 is the mean clutter reflectivity. The mean clutter power is given by equation (2.1) where the shape parameter is related to the sea clutter mean power by $p_c = v/b$.

2.4.4 Mean clutter reflectivity σ^0 models

The RCS of the clutter return per unit area is defined by the area reflectivity σ^o[2]. For a surface area illuminated by the radar resolution cell, the RCS of the clutter is determined by multiplying the illuminated area by the mean clutter reflectivity. The always changing and complex nature of the sea surface implies that the RCS of the return will fluctuates widely around the mean value as determined by σ^o.

A few models to determine the mean clutter reflectivity (RCS), σ^0, can be found in literature. These models have been developed by analyzing the scattering from the ocean surface [9]. RCS depends on a number of conditions such as the sea state, the grazing angle, the aspect angle with respect to the wind. Examples of such models includes, the GIT (Georgia Institute of Technology) model [2], The TSC (Technology Service Corporation) model [5] and a model developed by the Royal Radar Establishment (RRE) in the United Kingdom [2].

The GIT (developed for frequencies 1-100GHz) model, which is the most widely model used in the simulation of sea clutter, combines empirical factors with mathematical models. This model is as a function of grazing angle, wind speed, average wave height, wind direction, radar wavelength and polarisation. This model is currently known to be one of the best to provide a complex description of the ocean condition [2]. This is presented in Appendix B.

2.5 Coherent properties of radar sea clutter

There is a need for a concise characterisation of the Doppler spectrum of sea clutter so as to allow for a more general performance prediction to be made. Coherent radars employing Doppler precessing can distinguish targets from clutter if the target's radial velocity is sufficiently high [15]. However, some targets of interest will have Doppler shifts that are not significantly different from the Doppler spectrum of the clutter. In this case, it is important for the radar designer to have a detailed understanding of the characteristics of the Doppler spectrum for all different conditions likely to be encountered [7].

The temporal variation of the clutter is integrally involved with the simulation of sea clutter. The intensity of the clutter varies for the duration of observation. This variation needs to be characterised.

In coherent sea clutter simulation one is intending to match the statistic of the clutter in the time Domain as well as the intensity distribution within the Doppler domain.

Researchers for some time now, have been looking at characterising this coherent behaviour of sea clutter [10, 26, 15]. The major goal in sea clutter simulations is to be able to generate large surrogate data for the simulation of coherent sea clutter data. To generate coherent sea clutter, one aims at matching the statistics of real clutter in the time domain, as well as the shape and intensity distribution within the Doppler domain [10]. The simulation of realistic Doppler spectra has recently been reported in [26] and [10]. Recently, Watts [15] developed a new method for the simulation of coherent sea clutter. This method was able to show the temporal variation of the local spectra and the spiky characteristic of the amplitude statistics observed.

Figure (2.8) shows an example of a typical Doppler spectrum for sea clutter. This is the time history of the coherent spectrum from a single range cell, obtained from an S band radar. Each spectrum is generated from a 64-point Fourier transform. The polarisation is vertical and the sea state observed to be 4. From this figure the modulation of the intensity can be observed. Also, the spectrum has changing shape. As observed from Figure 2.8 there is a strong DC line and a very high Doppler frequency content appearing at 100 Hz. Comparing this spectrum to early NetRad recording as published by Inggs et al [4] there are some observed differences in the Doppler spectra obtained.

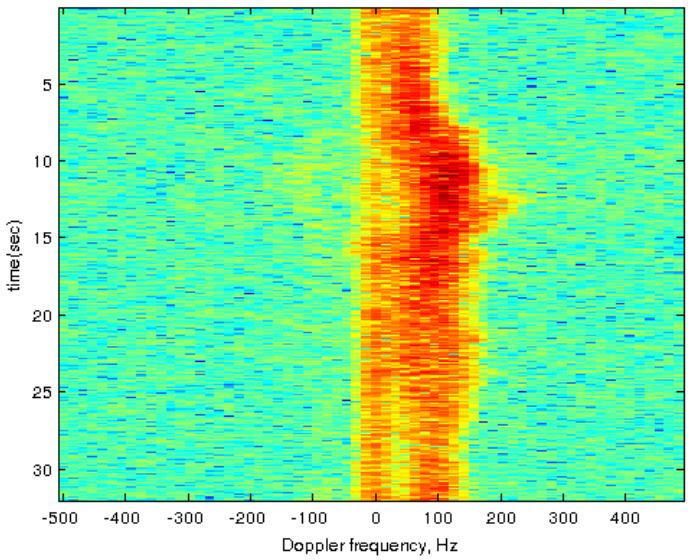

Figure 2.8: Time history of sea clutter Doppler spectra, from a single range cell. (Obtained from NetRad data set Inggs et al.[4])

These are the features that one aim to reproduce in the simulation of sea clutter [15]. The main advantage of understanding the coherent behaviour of sea clutter and being able to simulate the different Doppler spectra corresponding to different conditions is that it can help to separate out the bulk of the sea clutter returns when searching for small targets on the sea.

2.6 Summary

This chapter has briefly presented a few aspect of the analysis and simulation of sea clutter as seen in literature. The choice of the amplitude distribution used in characterising the clutter return as seen by a radar has been discussed together with different models used to define the mean clutter reflectivity. Also presented is the simulation of coherent sea clutter, how from the Doppler spectrum the temporal variation of the clutter can be observed.

Chapter 3

Simulation of Sea Clutter Returns

3.1 Overview

This chapter dwells on the simulation of sea clutter returns. It is divided into two sections. Section (3.2) presents a method by Tough and Ward [1] that is used to generate correlated K distributed random numbers with a specified correlation function. This is used to model the amplitude statistics of sea clutter. Section (3.3) presents a recently developed method by Watts [15]for the simulation of coherent sea clutter showing the temporal variation of sea clutter. These models are adapted and used in this dissertation.

The compound K distribution which is the most widely used probabilistic model for sea clutter analysis and simulation will be used to generate sea clutter amplitude statistics. The temporal properties of sea clutter as well as the Doppler spectrum as recently presented in [15] will be presented.

3.2 A method for the generation of correlated K distributed random numbers

As the observation of sea clutter deviates from the Rayleigh distribution for high radar resolution and low grazing angles, the K distribution helps to better predict the amplitude statistic of sea clutter. From Chapter (2), it was noted that the K distribution consist of two components. The local power of the clutter which can be modelled by the gamma distribution while the exponential distribution can be used to model the speckle component of the sea clutter. In many circumstances, the correlation properties of the more slowly varying gamma component of the clutter is the one that often affects the radar performance [1]. For simulation purposes and to have a good understanding of this phenomenon, there is a need to generate gamma distributed random processes with prescribe correlation properties. Unlike the Gaussian process that its linear transformation yields a Gaussian process, the linear transformation of the gamma processes may not generate a process that has the same properties. The Memory Non-linear Transform (MNLT) will be used in the dissertation. This method as presented by Tough and Ward [1] ensures that the gamma processes at the end has the required correlation properties as intended.

3.2.1 The memoryless non-linear transform

The memoryless non linear transform (MNLT) provides a map to transform samples from a zero-mean correlated Gaussian process to the desired gamma distribution with the desired correlation function. This is defined by equating the cumulative distribution function of a zero mean unit variance Gaussian process, evaluated at the value x taken by this process with the cumulative distribution of the required process [1].

If the required PDF is given by $P_{dist}(\eta)$, then

$$\int_{\eta}^{\infty} P_{dist}(\eta')d\eta' = \frac{1}{\sqrt{2\pi}}\int_{x}^{\infty}\exp(-x'^2/2)dx' = \frac{1}{2}erfc(x/\sqrt{2}) \tag{3.1}$$

Where $\frac{1}{2}erfc(x/\sqrt{2})$ is the complementary error function.

For the gamma distribution whose PDF is given in Equation (3.2), $P_{dist}(\eta)$ can be replaced with

$$P_c(x) = \frac{b^v}{\Gamma(v)}x^{v-1}\exp(-bx) \tag{3.2}$$

Since the MNLT performs a mapping via the cumulative distribution function (CDF) χ between the Gaussian and gamma distribution, then a zero-mean unit Variance Gaussian variate x'can be transformed via the CDF point α into a gamma variate

$$\int_0^x \frac{b^{2v}}{\Gamma(v)} x^{v-1} \exp(-b^2 x) dx = \alpha = \frac{1}{\sqrt{2\pi}} \int_{-\infty}^{\infty} \exp(-x'^2/2) dx'$$

Thus

$$x = \chi^{-1}_{gamma}(\alpha)$$

The x variates now follows the required gamma distribution.

3.2.2 Generation of correlated Gaussian random samples

An important step in the generation of correlated K distributed random variates is to first determine the correct correlation of the Gaussian samples before applying the MNLT [2].

By subjecting a Gaussian process to any linear operation for example filtering will yield a Gaussian process but with a different mean, variance and correlation function. The effect of the linear operation can be seen in the correlation properties of the output process.

Here, in this dissertation, the Fourier synthesis method of random processes has been applied in the generation of correlated Gaussian random samples with prescribed correlation function [2, 27, 28]. Consider the application of a filter to:

$$\phi(t) = \int_{-\infty}^{\infty} h(t-t')f(t')dt'$$

The correlation function of this process can thus be evaluated as such:

$$< \phi(t)\phi(\tau+t) >= \int_{-\infty}^{\infty} dt_1 \int_{-\infty}^{\infty} dt_2 h(t-t_1)h(t+\tau-t_2) < f(t_1)f(t_2) >$$

$$= \int_{-\infty}^{\infty} dt_1 h(t-t_1)h(t+\tau-t_1)$$

Or using Fourier transform the output of the filter gives us

$$\phi(w) = h(w)f(w)$$

The power spectra of the input and output processes related by

$$S_{\phi\phi}(w) = |h(w)|^2 S_{ff}(w)$$

A relationship between the auto-correlation function and the power spectrum of the output process

to the filter function can now be established. Therefore to reconstruct the process $\phi(t)$ the Fourier inversion can be applied. This is done by using the FFT algorithm.

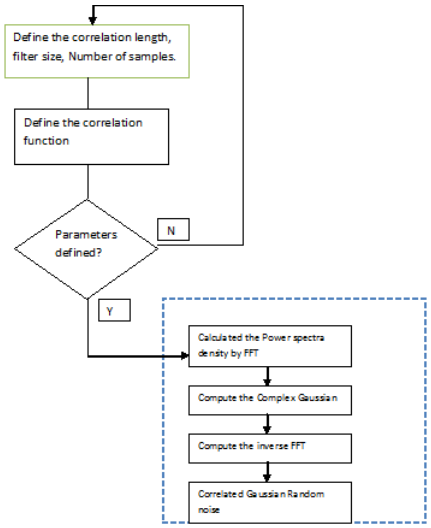

Figure 3.1: Flow chat showing the method used in generating correlated Gaussian random samples

The generation of correlated Gaussian samples was done as illustrated in Figure 3.1. Implementation of this process is available in program code. Refer to Appendix A for a detail description of the simulation package.

3.2.3 Generation of correlated gamma distributed random numbers by MNLT

Under the MNLT, by using correlated Gaussian variates as the input to the MNLT, the resulting gamma distributed variates will retain some correlation, but the auto correlation function (ACF) of the two will be different. The method of Tough and Ward [1] can be used to modify the input ACF to obtained the desired gamma ACF.

The steps describe here shows how to generate correlated gamma variates using the MNLT with the desired ACF Tough and Ward [1]:

- The first is to determine what kind of correlation function the required gamma distribution should have. If as an example the defined input correlation function is given as

$$< \eta(0)\eta(t) >= \exp(-t/\lambda)\cos(t/10)$$

  where λ is the correlation length, then using the method of Fourier synthesis [2] as described in Section 3.2.2 one can generate Gaussian correlated values that has the same auto correlation function (ACF) as the desired correlation function.

- To simulate realistic coherent sea clutter, the temporal correlation coefficient from a real radar data set will be used. This is determined by looking at the spectrum intensity of the real clutter data set for a specific range cell.

- Then, using this correlation function, N samples of correlated zero-mean, unit-variance Gaussian variates are generated. This is to ensure that the Gaussian samples are spaced as per the desired correlation function. Figure 3.2 is a plot of the desired ACF and the ACF of the correlated Gaussian before input to the MNLT method see Appendix C.

- Next, since the desired distribution is the gamma distribution, the correlated Gaussian variate is then transformed to gamma random variates. As explained in the section above, the MNLT maps this by equating both cumulative distribution together and solving for the required distribution. Then, by taking the inverse gamma cumulative probability density with the correlated Gaussian as input and the required shape parameter, the gamma distribution is obtained. Figure 3.3 shows the auto correlation of the Gaussian input to the MNLT and the resulting gamma ACF. It is observed that the resulting gamma ACF follows the desired correlation function.

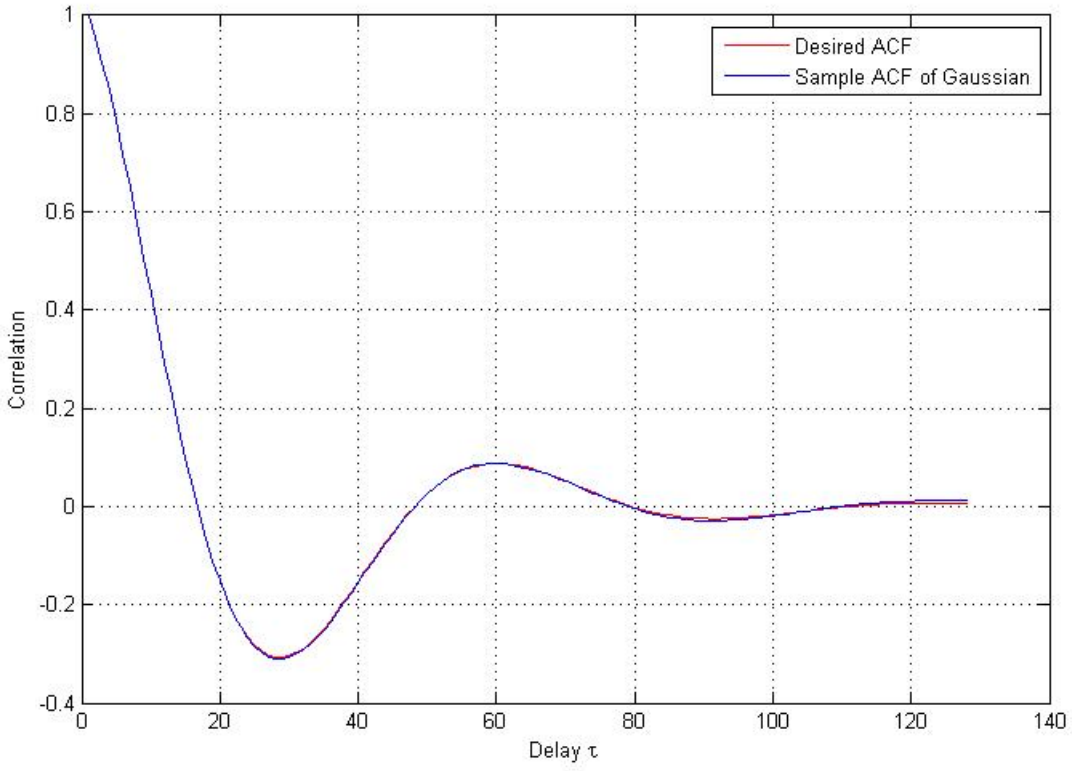

Figure 3.2: The auto correlation function of the desired and the sample Gaussian distribution

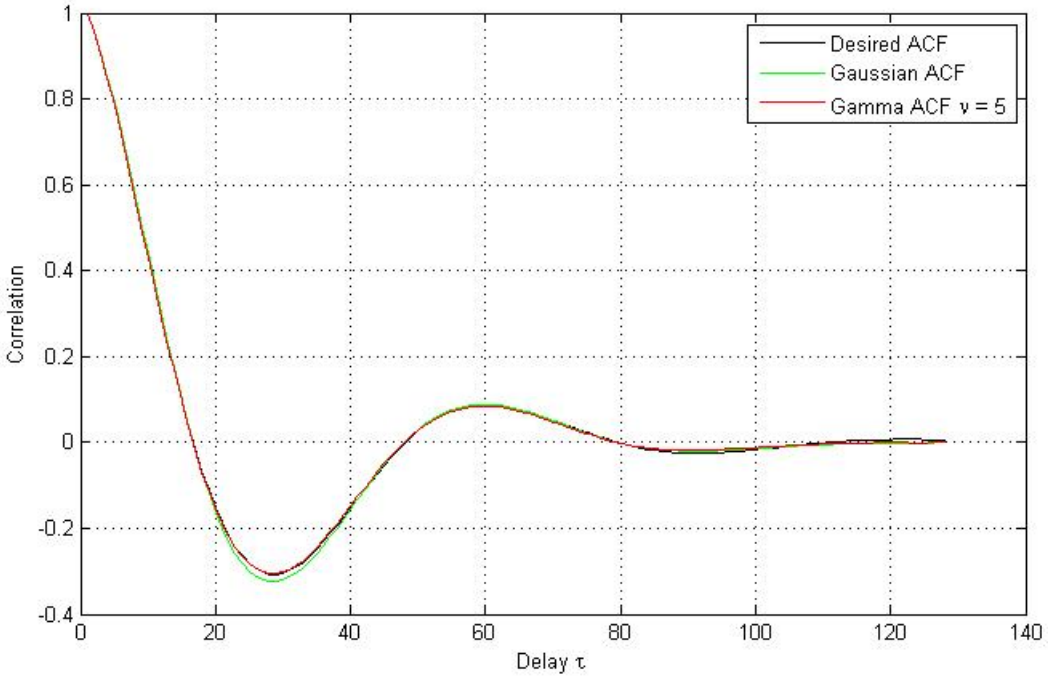

Figure 3.3: The auto correlation function of the desired, Gaussian and the resulting Gamma distribution.

3.2.4 K distributed random variates

The K distribution is determined by modulating the correlated gamma random variates with an exponential distribution. As the gamma distribution models the local power of the sea clutter, the exponential distribution is used to model the capillary waves also often called the speckle components. Thus by multiplying the local power and the speckle component, one can generate the K distributed clutter.

Figure 3.4 shows the K distributed random variates generated by using the MNLT method.

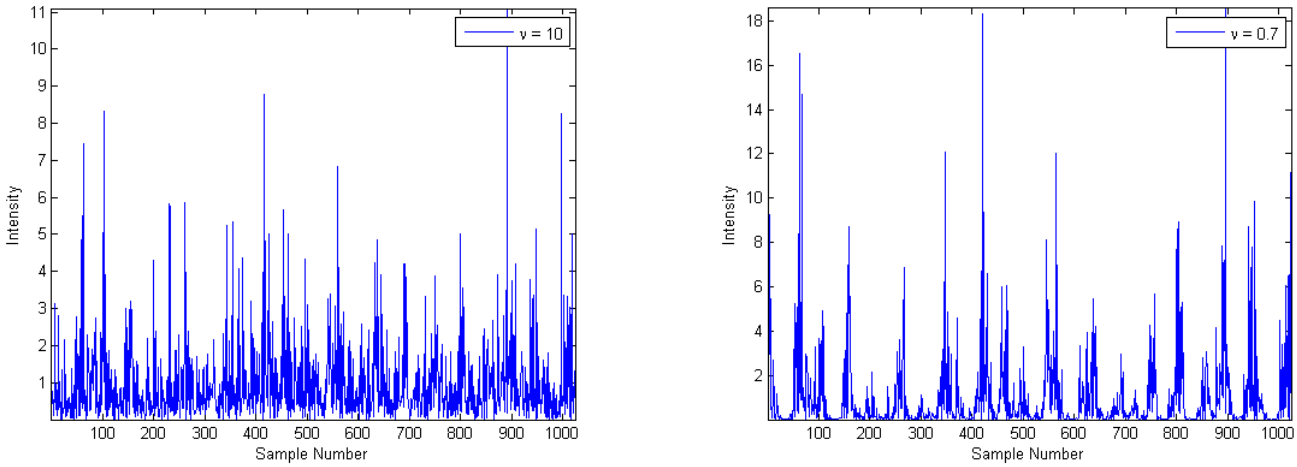

Figure 3.4: K distributed random variates for different values of shape parameter v with b =1

3.3 Simulation of coherent sea clutter

As mention earlier, the ability to be able to simulate Doppler spectra and to model the temporal correlation of sea clutter is very important in understanding behaviour of sea clutter. The radar returns from the patch of sea illuminated is usual not independent from pulse to pulse. The variation of the clutter from a single range cell over the time of observation Needs to be modelled [26]. If a targets radial velocity is higher than that of the clutter, then the clutter effects might not really be a problem, but in cases where the clutter radial velocity is much higher than the targets, the target can be mistaken for clutter.

In this section, a method recently developed by Watts [15] describes a technique for modelling and simulating the coherent returns from radar sea clutter, based on the compound K-distribution model for clutter amplitude statistics. By using the observation of a recorded radar data's spectra one can characterise the temporal variations of the Doppler spectrum observed in a single range cell.

This method is described as follows:

- The spectra are assumed to have a Gaussian-shaped PSD of the form:

$$G(f,x,s) = \frac{x}{\sqrt{2\pi}s} \exp\left[\frac{-(f-m_f(x))^2}{2s^2}\right]$$

where

f	:	Doppler frequency
$m_f(x)$	:	mean Doppler frequency
s	:	Spectrum width

The mean Doppler frequency as a function of x is obtained by analysing the radar data set and determining a least mean square error straight line fit to the data.

- The spectrum width, s, is assumed to have a PDF as a Normal PDF of the form:

$$p(s) = \frac{1}{\sqrt{2\pi}\sigma_s} \exp\left[\frac{-(s-m_s)^2}{2\sigma_s^2}\right];\ 0 \leq s \leq \infty$$

m_s : Mean spectrum width
σ_s^2 : Variance of spectrum width

- Using the method for the generation of correlated gamma distributed random variate of Section 3.2.3, the time varying local mean intensities of the spectra are generated as M gamma distributed variates, x_m, with shape parameter v, and spaced in time by L/f_r having the same correlation coefficient over the original data. L is the FFT length and F_r is the pulse repetition frequency of the radar.

- Next, generate a set of L complex variates, g_l, with in-phase and quadrature components having a independent Normal distributions N[0 1] for each value of the local intensity, x_m.

- These are then weighted according to appropriate sampled spectrum by $\sqrt{G\left(l\left(F_r/L\right), x_m, S_m\right)}$

- Thermal noise is then added as complex Normal variates to give the required clutter-noise-ratio.

Apart from simulating discrete spectra as describe above, there is also the possibility of simulating a continuous time series with the right Doppler characteristics as explored in Watts [15].

The flow chat in Figure 3.5 summarises the processes given here for the simulation of the Doppler spectra having temporal properties as that observed from a real sea clutter radar measurement.

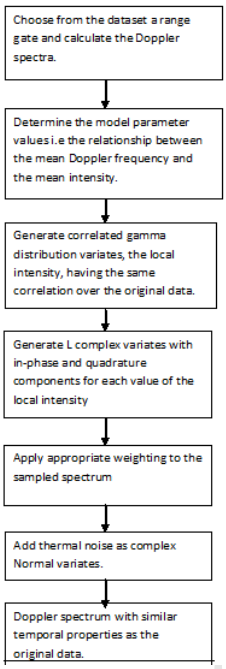

Figure 3.5: Flow diagram showing the algorithm for the simulation of sea clutter Doppler spectra

3.4 Summary

This chapter presents a methodology for the simulation of non-coherent and coherent sea clutter. These methods which were recently developed will be used in this project to simulate the amplitude characteristic of sea clutter as well as an attempt to simulate the temporal variation of the clutter as observed by the NetRad radar data.

Chapter 4

Simulation of Sea Clutter Returns - Amplitude Statistics

4.1 Introduction

This chapter mainly deals with the analysis of the simulated sea clutter amplitude statistics. The simulation procedure used to generate correlated K distributed random variate given the sea state, environmental conditions and the geometry is presented. The main goal in the simulation of sea clutter is to be able to generate sea clutter data with amplitude statistics that can be compared to that as observed by a radar system. As explained in Chapter 2, the K distribution is best know to effectively model sea clutter. As such, the simulator is based on the K distribution.

Evaluation of the results obtained from the output of the simulator is presented. Statistical goodness fit test was carried out using the Kolmogorov–Smirnov (K-S) [29] single point test method as well as fitting the simulated correlated K distribution variates to the theoretical PDFs.

4.2 Implementation of sea clutter simulating procedures

The simulator is written in MATLAB® using the methodology for the generation of sea clutter amplitude statistics as presented in Chapter 3. The implementation procedure of various function of the simulator is presented in Appendix A.

A typical simulation scenario is shown in Figure 4.1. Here the radar is placed on a cliff top looking out towards the sea. This schematic presents the parameters that are needed for the simulation of sea clutter returns. These parameters includes the radar frequency, transmitted power, bandwidth, grazing angle, polarisation antenna gain. Also needed are environmental factors such as the sea state and swell direction relative to the wind direction. All these parameters should be defined in various sub routine to commence the generation of sea clutter that is, correlated K distributed random

variates with a prescribe correlation function.

Here, only the amplitude characteristic of sea clutter is explored for a given weather, environmental conditions as well as radar parameters. The temporal properties of sea clutter will be discuses in Chapter 5 as seen from the Doppler-Time plot of the experimental radar system NetRad [4] sea clutter measurements.

The block diagram in Figure 4.2 shows the order of calling of the procedure for the generation of the K distribution shape and scale parameters. The order in which these are determined are presented is presented as follows;

Prediction of the average radar cross-section per unit area σ^o using the GIT model.

This first step is to predict the mean radar cross section σ^o (also known as the mean reflectivity) of the illuminated patch of the sea. This represent the mean value of the clutter of which the instantaneous power received from a single radar resolution cell varies about this mean value. This variation cames about as a result of the variation of the local surface shape, grazing angle, ripple density, and other factors associated with the passage of long waves and swell, cause the backscatter from an illuminated patch to vary about the mean radar cross section. Also, within a radar resolution patch, scattering occurs from many small structures which move relative to each other and create interference in the scattered signal [2].

The radar cross section (RCS) is gotten my multiplying the illuminated patch area, A, by the predicted mean radar cross section for a forecast weather and environmental condition.

Using the GIT model [2] given in section B, σ^o value is determined. The Matlab routine for this is as follows.

The inputs required are:

- The sea state. This is determined by using the Douglass table [5] as seen in Table 2.1. This is a numerical representation of the roughness of the sea. Sea state 1 represents a very calm sea with very little or no noticeable clutter while sea state 6 represent a very rough sea with wave heights reaching up to a few meters. This is very much dependent of the wind speed.

- The grazing angle. This is the angle the illuminating electromagnetic wave makes with the sea surface.

- The radar's wavelength as determined from the radar frequency.

- The Polarisation of the radar transmitter and receiver.

Prediction of the K-distribution shape parameter, v, using an existing empirical formula by Ward et al. [2].

The empirical formula as seen in Equation 2.7 can be used to predict the K distribution shape parameter. This is dependent of illuminated area, the grazing angle, the polarisation used and the swell direction. The gamma PDF requires this parameter as the gamma distribution is characterised by both the shape and the scale parameter. This value is determined taking in as inputs the grazing angle, the radar resolved area, the polarisation and computes the shape parameter.

The shape parameter gives information about the amplitude statistics. Small grazing angle results in smaller shape parameter as evident from Equation 2.7.

Calculation of the average clutter power at the receiver according to the radar equation.

To calculate the clutter power at the receiver Equation 2.1 is used. This is used to determine the clutter power given the radar cross section area, σ^o, the radar antenna gain, the illuminated area, loses in the system comprising of the microwave losses, and the range. Also with the knowledge of the clutter power, the clutter to noise ratio (CNR) for a particular radar measurement can be determined.

Calculation of the K distribution scale parameter b using the relationship between the K distribution shape parameter and clutter power at the receiver.

The next step is to determine the K distribution scale parameter using this relationship $p_c = v/b$. Here p_c is the average clutter power and b is the scale parameter.

Generate correlated K distributed random variate

Once the gamma PDF scale and shape parameter has been determined, the next step is to generate N number of correlated Gaussian random variate (Refer to ref [30]). From the method as presented in section 3.2.3, the underlying sea clutter modulation follows the gamma distribution and to generate the required correlated gamma distributed variates, correlated Gaussian variates are first generated and then transform to gamma PDF.

The correlated K distributed random variate is then obtained by modulating the correlated gamma random variates with an exponential distribution.

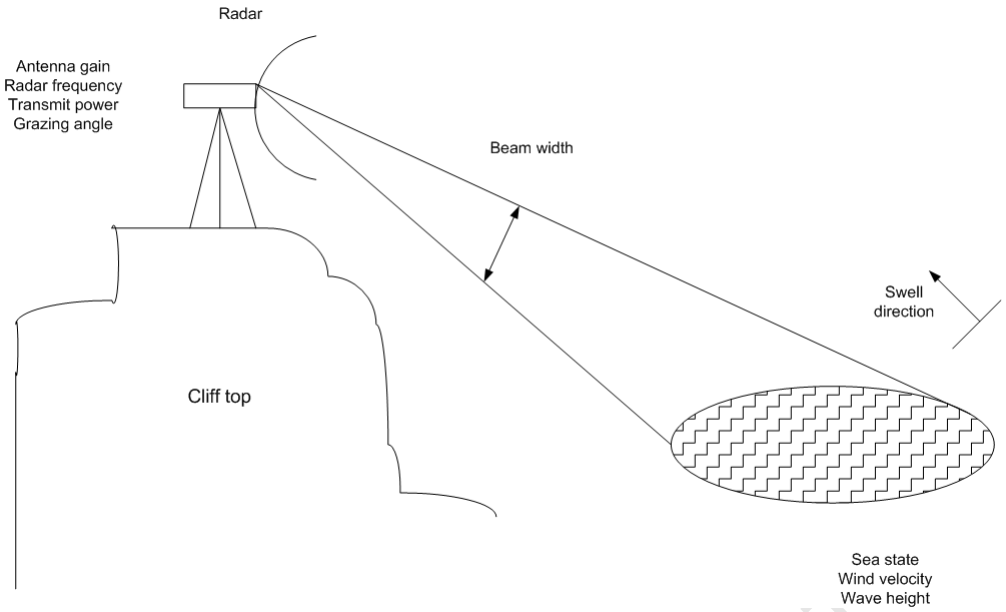

Figure 4.1: Typical simulation scenario

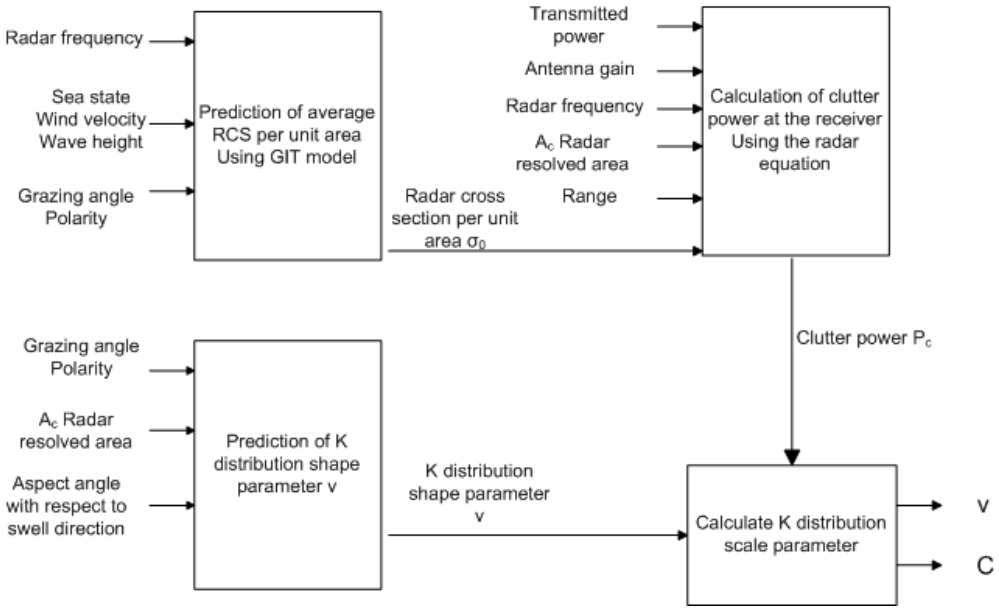

Figure 4.2: Block diagram showing the simulation procedure for the generation of the K distribution shape and scale parameter

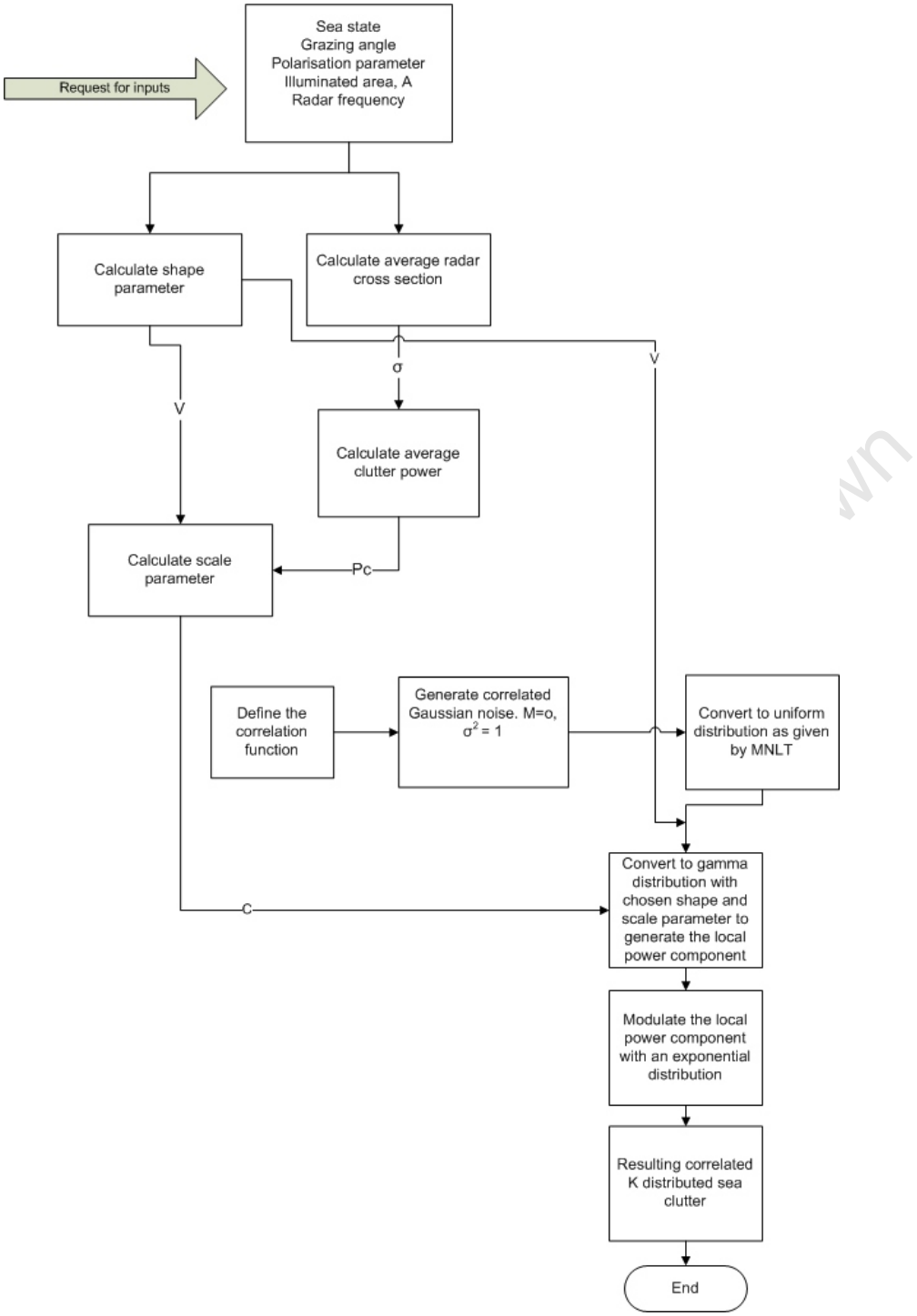

Figure 4.3: Flow chat showing simulation procedure

The flow chat in Figure 4.3 summarises the process for generating correlated K distributed random variates. Making use of the shape and scale parameter, the MNLT is used to generate correlated gamma variate with prescribed correlation function. Afterwards, the correlated gamma variate is modulated with an exponential distribution to yield the correlated K distribution.

4.3 Results and Verification

The verification of the results obtained from this simulation will be in three parts. First, the amplitude statistic of sea clutter as the shape parameter changes will be investigated the reason been that the shape parameter tells how spiky the clutter will be. Secondly, the K distribution probability density function model will be fitted to the generated correlated random K distributed variates to verify whether the PDF of the clutter generated matches the PDF of the prescribed function or not. Thirdly, the K-S single point statistic test will be carried out on the correlated variates.

4.3.1 Varying shape parameter *v*

As mention in section 2.4.2, the shape parameter *v* is one of the parameters that describes the K distribution. Its value is used to predict the amplitude of the clutter. Figure 4.4 shows the simulated correlated K distribution random variates for various shape parameter keeping the scale parameter constant 'b'. This was done by changing the value of the shape parameter *v* in the simulated procedure. The graphs are then plotted for different values of v/b, the mean intensity.

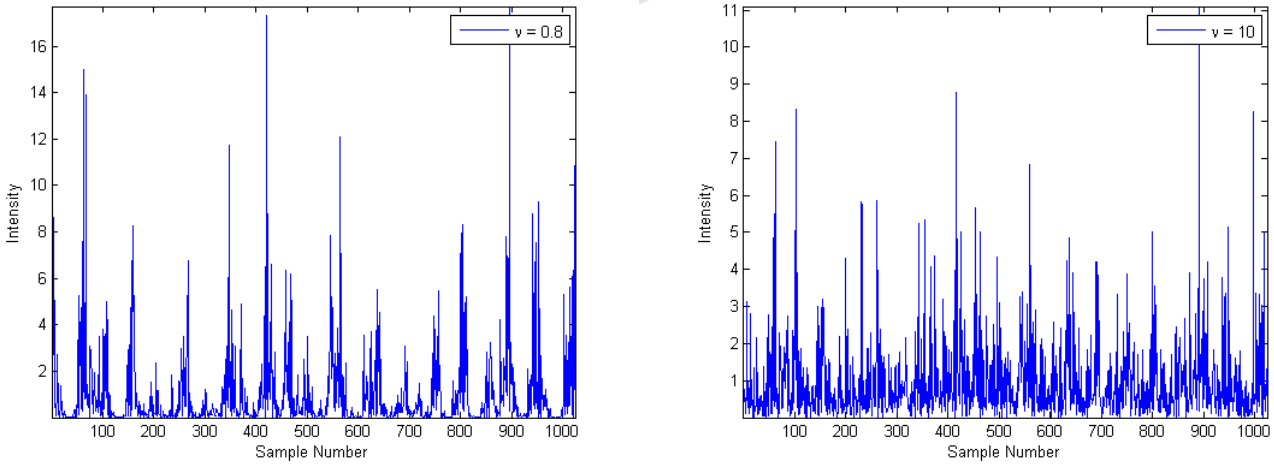

Figure 4.4: Correlated K distributed random variate for various value of shape parameter with unit scale parameter

As can be observed from Figure 4.4, the peak values increases relative to the mean value for smaller values of *v* than it is for larger ones. Therefore, for higher sea state value (rougher sea) the clutter spikiness increases. This is as expected and conforms with the literature.

4.3.2 Fit to the K distribution

The generated correlated random variates were fitted to the K PDF. This was done by estimating the histogram of the amplitude of the generated clutter data and comparing with the theoretical K dis-

tribution PDF. Using the Method of Moments (MoM) the estimated and theoretical moments up to order 6 was calculated. Figure 4.5 shows the PDF of the generated correlated K distributed random variate fitted to the theoretical K PDF. By inspection, it can be observed that the theoretical K distribution fits best the generated correlated K distributed variate. The normalised moment versus the moment order of the simulated correlated random variates are plotted in Figure 4.6. For comparison, in the same figure, the theoretical moments for the Lognormal, Rayleigh, Weibull and K distribution are reported. The data shows a good agreement with the K distribution although the Weibull also shows a good fit.

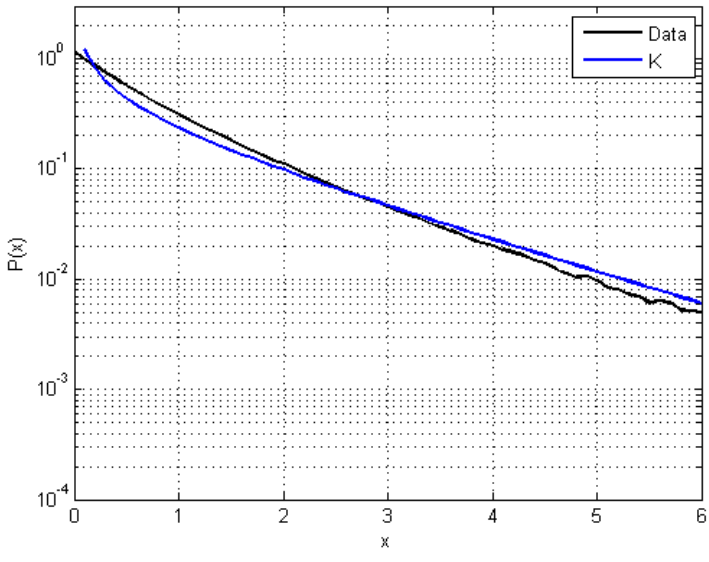

Figure 4.5: Shows the PDF of the generated correlated K random variate fitted to the theoretical K PDF

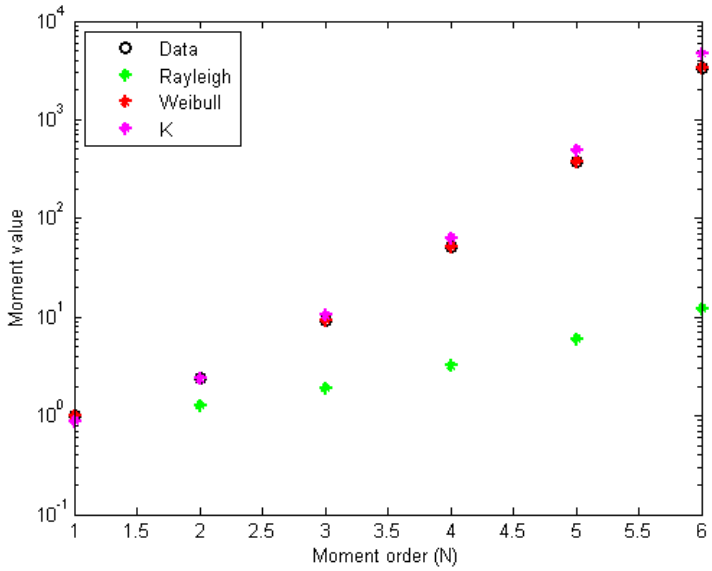

Figure 4.6: Normalised moment versus moment order

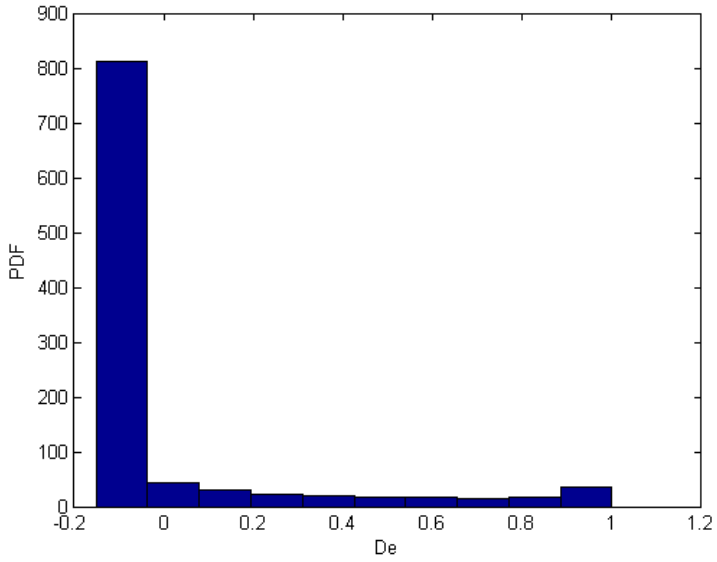

Figure 4.7: The probability density function for D_e values of the Kolmogorov-Sminov test

4.3.3 Kolmogorov–Smirnov test

To determine whether the amplitude data generated indeed arises from the K distribution, the K-S test is performed. This is a non-parametric test for the equality of continuous, one-dimensional probability distributions. The K-S statistic quantifies a distance between the empirical cumulative distribution function (CDF) of the sample and the CDF of the reference distribution.

$$D_e = \max |F(x_i) - F_t(x_i)| \tag{4.1}$$

where $F(x_i)$ is the empirical CDF and $F_t(x_i)$ is the theoretical CDF for the K distribution.

D_e can be compared against the critical value D_{crit} given by Papoulis [31]. If D_e is greater than D_{crit}, then the null hypothesis can be rejected and the data cannot be said to have arisen from the same distribution. From the simulated correlated K distributed clutter the K-S test has been performed. For a significant level of 0.05, $D_{crit} = 0.1055$ and from Figure 4.7, which was also recently published in [32], it can be observed that most data have values smaller than D_{crit}.

Further analysis was carried out in other to establish a trend in the simulation results. Different values of the K distribution shape parameter was used to generate the clutter and K-S test was carried out by computing the maximum of the different of the CDF between the two curves as given by Equation 4.1.

Here, different values of v (shape parameter) will be tested. In Table 4.1, h indicates the result of the null hypothesis. h = 1 if the test fails the null hypothesis with a 5% significance level and h = 0 otherwise. k gives the test statistic of the maximum difference between the two CDF curves. P is the asymptotic p-value.

Table 4.1: Table showing results obtained from the K-S test of different data corresponding to different K distribution shape parameter

Shape parameter	h	p	k
v = 0.7	0	0.9076	0.1058
v = 5	1	5.6376e-19	0.8662
v = 10	1	3.1630e-23	0.9603
v = 0.8	0	0.6846	0.1342

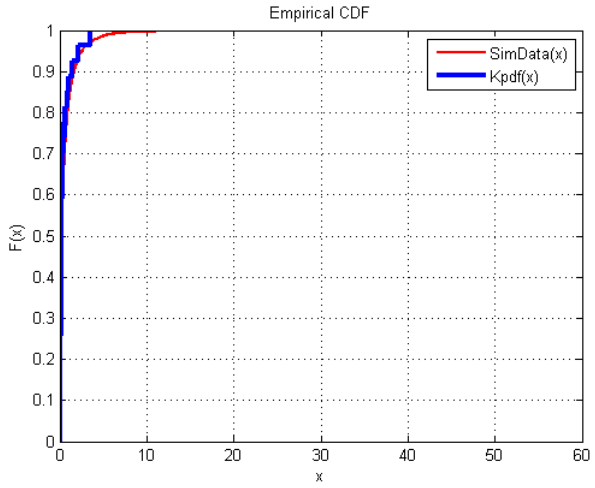

Figure 4.8: The K-S test for K distribution shape parameter v = 0.7

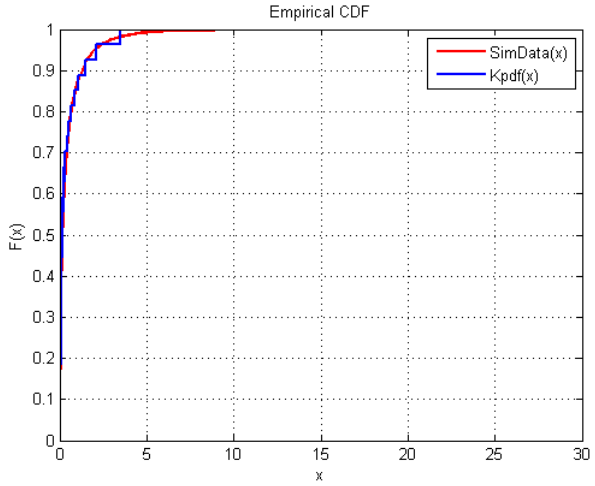

Figure 4.9: The K-S test for K distribution shape parameter v = 0.8

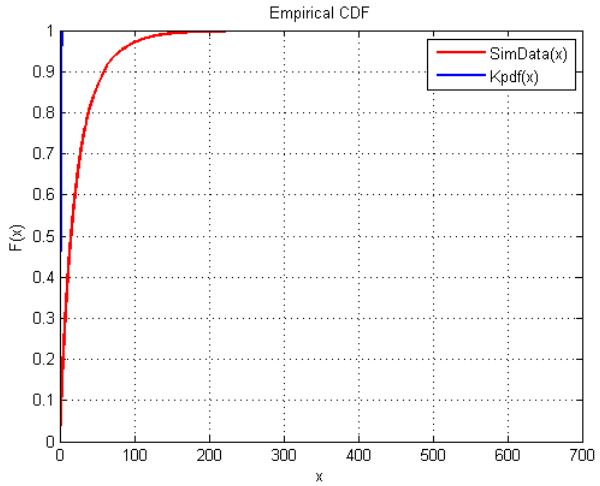

Figure 4.10: The K-S test for K distribution shape parameter v = 5

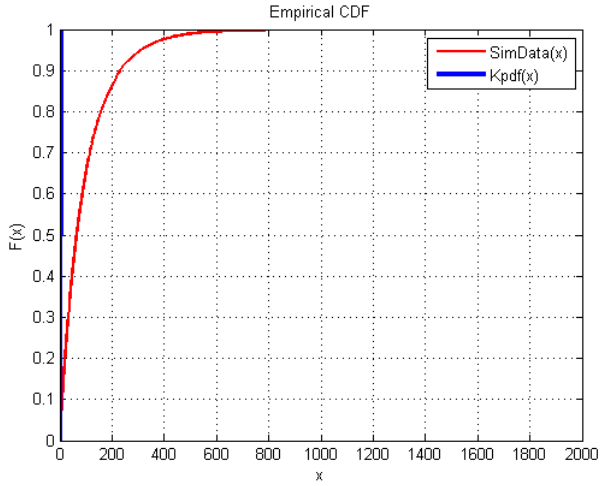

Figure 4.11: The K-S test for K distribution shape parameter v = 10

It can be observed that the null hypothesis passed for smaller values of the K distribution shape parameter but fails for higher value. These trend shows that for the simulator output having smaller value of shape parameter, i.e very spiky clutter, the results passes the K-S test while for larger values of the shape parameter, the test fails the null hypothesis. In such cases, further analysis would have to be carried out.

4.4 Summary

This chapter has described the use of the memoryless non-linear transform to generate correlated K distributed variates from a given auto correlation function. The K distribution function very well explains observed experimental data.

From the fit of the simulated correlated K distribution random variates to the theoretical K distribution, results obtained shows that there is a good fit. The K-S test has been shown that the simulated clutter follows the K distribution. Plots showing the fitting of the theoretical PDF to the simulated random variates provides a visual indication of a good fit.

Chapter 5

Experimental Measurements

5.1 Introduction

This chapter deals with the analysis of experimental measurements carried out using the NetRad system [4]. This analysis here is done by fitting the amplitude distribution of the clutter to the K distribution PDF and as well as plotting the Doppler spectrum of the clutter to observed the temporal variation of the clutter and to determine what model will best fit the spectrum. All the measurements used in this Chapter and dissertation were obtained from the Monostatic node of the NetRad system. Only monostaic sea clutter was considered.

The Netted radar experimental radar system is first introduced with the environmental set up for the experiments followed by the data analysis of sea clutter measurements.

5.2 NetRad

NetRad is a muiltistic netted radar system. The radar system comprises of several nodes that are spatially separated. Designed by University College London (UCL) in collaboration with the University of Cape Town (UCT), the system parameter are summarised in the Table 5.1.

Table 5.1: NetRad system specification

Parameter	Value
Carrier frequency	2.4 GHz
Transmit power	500 W (one node, others 200 mW)
Range resolution	3m
waveforms	Arbitrary linear FM and Polyphase
pulse length	0.1 - 10 μs
PRF	50 Hz - 2 kHz
Bandwidth	45MHz

The transmit frequency is 2.4 GHz which is in the unlicensed band. The antennas are 94cm in diameter providing a gain of approximately 24dBi with $8^{o}X\,8^{o}$beam-width. The overview of the design of this system can be found in references [33, 34, 35, 4, 36].

Figure 5.1 shows the experimental set up of NetRad radar system to measure sea clutter. The antennae are mounted along the coastline pointing towards the sea. Several sets of measurements were done for different azimuth and elevation angles and also for different polarisation. The radar is capable of bistatis/tristatic sea clutter measurements with receiving node 1 and 2 and the transmitter receive pair node 3 placed at different locations to give the bistatic angle required. For different desired pulse length, the radar transmit at 2.4 GHz frequency with peak power of 200mW.

Measurements taken for the data set used in this analysis was done at Scarborough cape Town. With the transmitter and receiver node 3 place at Misty Cliff and the receiver node 1 and 2 placed some distance apart. Figure 5.2 shows a google earth image of the location. Only the monostatics data, that is, from receiver node 3 will be considered in this project.

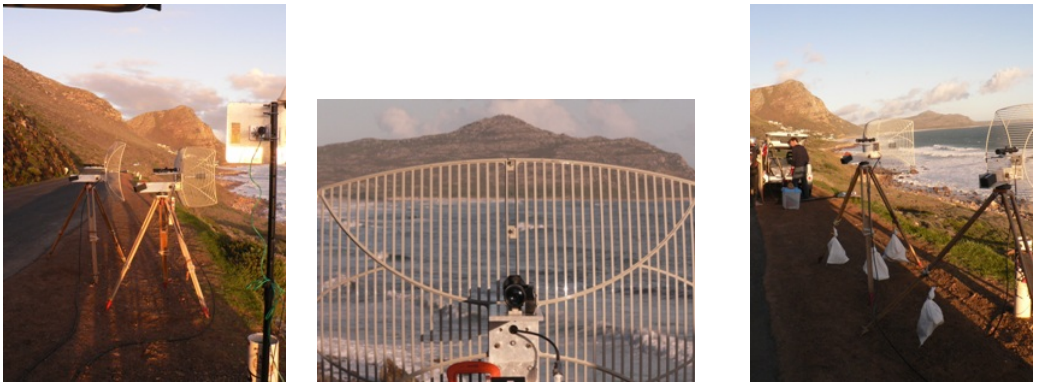

Figure 5.1: NetRad experimental set-up Scarborough Cape Town

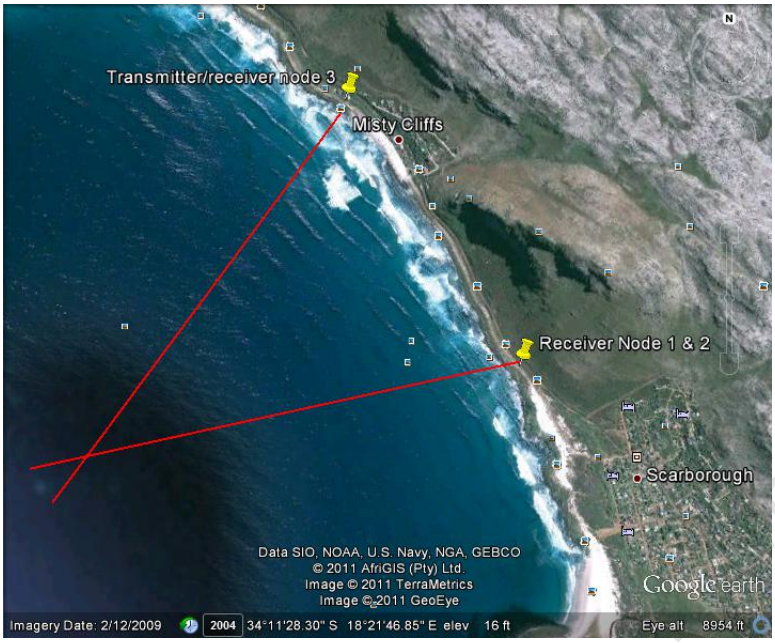

Figure 5.2: Google earth image of the experiment site

5.3 Data analysis and modelling

This section presents the analysis of the radar sea clutter data. This analysis have been applied to other sea clutter data obtained from NetRad with similar results obtained, but the specific data set used to illustrate the result in this chapter was '11_06_05_1531_51_P1_1_32500_S0_1_8191_node3 - Node 3 Rx.mat. This was from the experiment done on the 5th of June 2011 at 15h31 at Scarborough Cape Town South Africa. A pulse length of 10μseconds was used with the radar transmit power set at 500 W. The mat file is from Node 3 which is the monostatic node.

The data set consisted of 32000 successive samples from a single range cell, representing a time interval of about 32 seconds. The radar was vertically polarised with transmit frequency of 2.4 GHz, a pulse repetition frequency of 1 kHz and range resolution of about 3m. The radar's local grazing was approximately 1 degree. The radar azimuth was set to 82.5^{o}and the elevation set to -1^o.

On that day the weather station report of Scarborough Cape Town wind speed was about 5.6 km/h and the wave height was about 3m [1]. Thus according to table 2.1 the predicted sea state was 3.

Hilbert transform was performed on the raw real data to get the complex envelope of the signal after which a match filter was applied using a 10 μs reference pulse. This are then stored in a Matrix in which the roles corresponds to the pulses number and the columns corresponds to the samples at different ranges.

Figure 5.3 shows the time history of the clutter amplitude from a single range cell for the data set described above. This clutter amplitude is taken from range cell 200 which from the range resolution

[1] http://www.wunderground.com accessed 5 November, 2011.

corresponds to approximately a distance of 600m from the radar. The presence of spikes are evident, also from the figure the amplitude variation of the clutter can be observed. Dominant spike persisted for about 4 seconds between 3-7 seconds.

In comparing the amplitude distribution of the clutter to proposed models in the literature, the data from the range cell was fitted to Rayleigh, K distribution and the Weibull PDF distribution. As seen in Figure 5.4, the data set shows to fit the K distribution well more than the Rayleigh distribution. Furthermore, the moments up to the sixth order was computed and compared to the theoretical K, Rayleigh and Weibull moments shown in Figure 5.5. The data shows a good agreement with the K distribution.

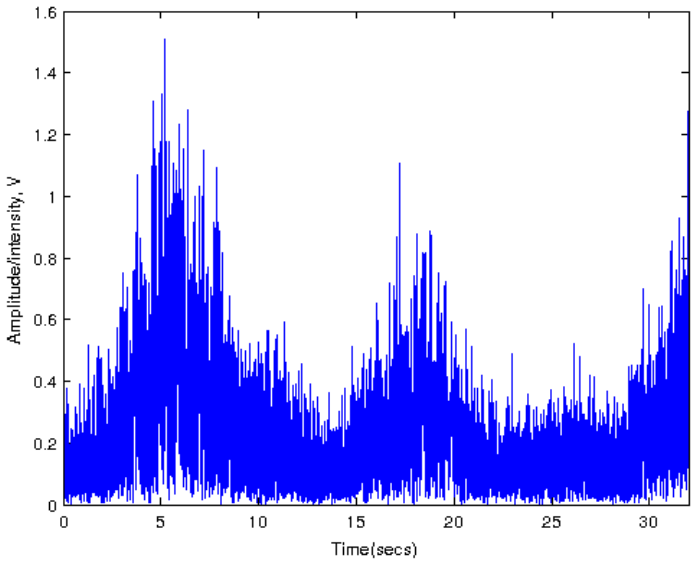

Figure 5.3: Time history of the clutter amplitude from a single range cell

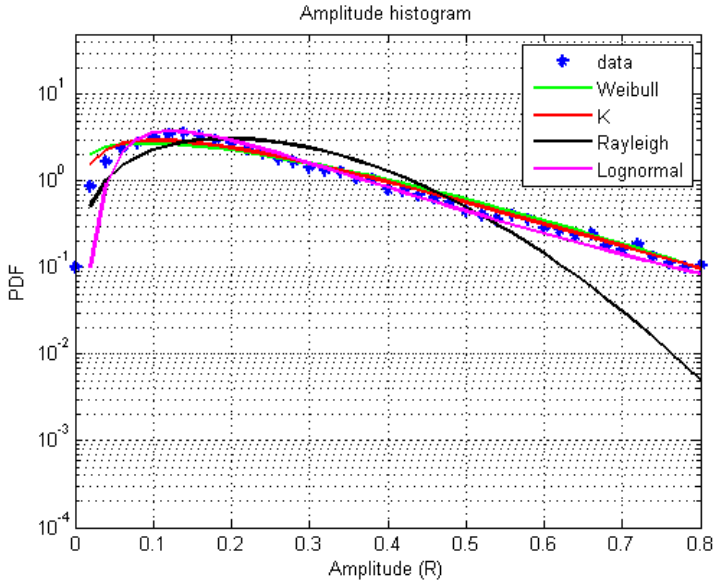

Figure 5.4: Amplitude histogram of the data fitted to different distribution

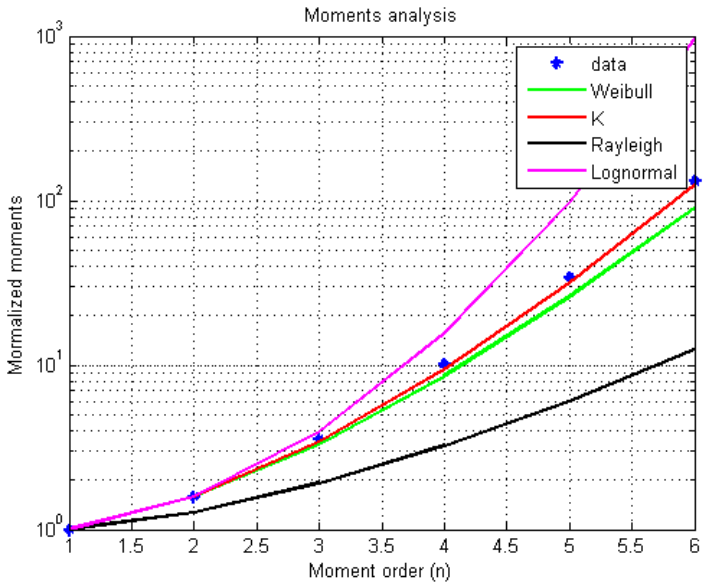

Figure 5.5: Normalised moment versus moment order

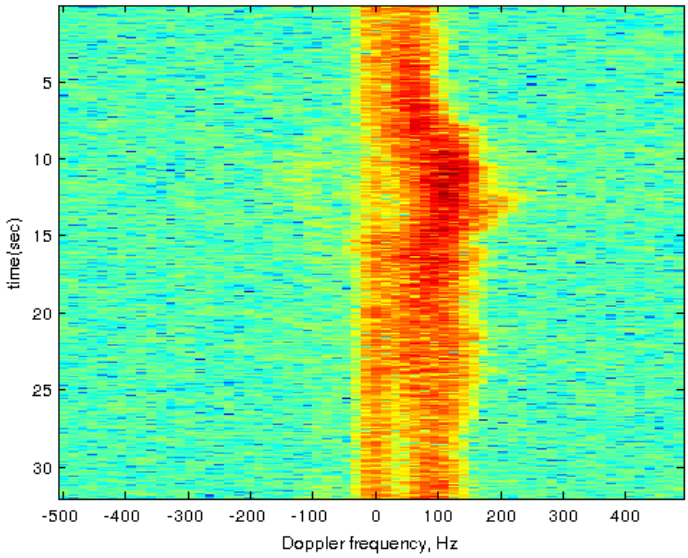

Figure 5.6: Doppler spectra (dB) from a single range cell; f_r = 1kHz, FFT length l = 64, -55 dB Doplh-Chebyshev window

5.3.1 The Doppler spectrum of sea clutter

To observe the temporal correlation of the sea clutter, the Doppler spectrum was calculated. This is to enable one to examine the intensity change of the clutter with time.

The raw data was the processed over a burst of L = 64 samples with a fast Fourier transform (FFT) and using a -55 dB Dolph-Chebyshev weighting function in the time domain. Figure 5.6 shows the power spectra density of the data for 500 successive spectra corresponding to 32 seconds. As seen, the spectrum width varies with time, with Doppler excursions as seen around 10 seconds which might be as a result of local wind gusting. Also noted is the asymmetric nature of the spectrum. Overall, the spectrum looks well-behaved, with a non-zero mean Doppler shift which appears to vary with time.

However, also observed from Figure 5.6 is a strong DC line and a very high Doppler frequency content appearing at 100 Hz. Comparing this spectrum to early NetRad recording as published by Inggs et al [4] there are some observed differences in the Doppler spectra. Figure 5.6 shows some unexpected artefacts round 7s and 12s. This is probably due to interference during measurements.

5.4 Summary

The NetRad experimental radar system was presented in this chapter. This is a netted radar system capable of synchronising multiple receiver and transmitter at different location. The sea clutter trails data collected by this radar was analysed. From the analysis, the statistic of the clutter return from a single range cell shows to fit the K distribution model. Also plots of the Doppler spectrum shows the temporal variation of the clutter with time.

Chapter 6

Conclusions

6.1 Summary

This section presents a summary on the work done in this dissertation.

A literature review on sea clutter simulation was presented. This reviewed classical approaches that are usually taken in the simulation of sea clutter. This is often done stochastically with the aim of matching the observed properties seen by a radar during sea clutter measurements. A description of the sea surface together with geometrical arrangements of a radar system measuring sea clutter was presented. Furthermore, the Dounglas table 2.1 which gives a description of various sea state as the wind speed changes was also presented. Some recently published work available in the literature were also reviewed showing the amplitude statistics of the clutter as well as the temporal variations of sea clutter and how these properties maybe reproduced by simulation.

A well known method developed by Tough and Ward [1] for the simulation of correlated K distributed random variates was investigated. The K distribution encompasses the gamma distribution which models the slow varying structure of the sea as well as an exponential distribution that models the fast varying component of the sea. The gamma PDF is characterised by its shape and scale parameter. Ward et al. [2] provides a method that takes into account the sea conditions as well as the viewing geometries of the radar to calculate the shape parameter. This method was used to generate the amplitude statistic of sea clutter in this dissertation.

Using this approach, a sea clutter simulator was developed for the amplitude statistic of sea clutter. This simulator was written in MATLAB® and makes use of the afore mentioned methods for the generation of correlated K distributed random variates. This simulator takes in as input weather conditions specifically the sea state, the geometry of the radar system as well as the radar parameters to calculate the mean clutter reflectivity, the shape parameter, and subsequently the scale parameter.

Sea clutter experimental measurements were carried out using the NetRad radar system. This is a netted radar system capable of synchronising multiple receiver and transmitter at different locations.

The received backscatter signal from the monostatic node of the radar from measurements done at Scarborough Cape Town was processed. A comparison of the PDF of the measured clutter and the theoretical K distribution PDF was done. Furthermore, a 64-point FFT was used in calculating and plotting the Doppler spectrum of the clutter from a single range cell to show the temporal variation of the clutter. The average spectrum fits the Gaussian model thus a Gaussian model can be considered in simulating the Doppler spectrum as observed by NetRad.

The temporal correlation of sea clutter was also addressed. The clutter as observed from an illuminated patch of the sea varies with time. This temporal nature is of importance in the simulation of sea clutter as well as in developing suitable signal processing techniques that helps in the detection of targets in clutter. A recent method developed by Watts [15] shows this temporal behaviour and presented a way of reproducing this observed properties. This method is presented in this dissertation.

6.2 Discussions and conclusions

This section presents discussions and conclusions on the different aspect of sea clutter simulation carried out in this dissertation.

6.2.1 Simulation of correlated K distribution random variates

In simulating sea clutter with prescribe correlation function there is the need for the ACF of the desired function to match that of the gamma ACF. This has been achieved in this dissertation. As shown in Figure 3.3 the gamma distribution has the desired correlation function after the transformation process. The gamma distribution is known to model the slowly varying component of the sea clutter (the gravity waves of the sea) and its correlation properties are taught to affects radar performance. Thus the importance of generating gamma distributed random processes with prescribe correlation properties. The gamma process is not linear unlike a Gaussian process which is linear. The use of the method by Tough and Ward [1] makes it possible to generate correlated gamma random variates with a prescribe correlation function.

Figures 3.4 shows the K distribution with specified shape and scale parameters generated by modulating the correlated gamma distributed random variates with an exponential function as required by the K distribution. The correlated gamma distribution represents the local power of the clutter while the exponential function gives the speckle component. From results shown in Figures 3.4 and 4.4, the underlying gamma random processes can be observed with speckle component as well as the underlying modulation.

Furthermore, statistics of goodness of fit test carried out on the amplitude distribution of the clutter proved that the simulated clutter amplitude statistic indeed arises from the K distribution. Figure 4.5

shows good fit of the theoretical K distribution PDF and that simulated.

For a rough sea, higher sea state, the clutter spikiness increases. This is evident from the empirical formula that describe the K distribution shape parameter. The variation of the sea state increases the clutter amplitude and vis versa as shown in Figure 4.4 thus agreeing with literature.

The Kolmogorov–Smirnov test was carried out to further verify the outcome of the generated random variates. The test shows that the random samples results from the K distribution for smaller values of the K distribution shape parameter. Visualisation plots of the PDF shows good fit as seen in Figure 4.7.

6.2.2 Experimental results

The analysis of the experimentally collected data from NetRad system shows that the K distribution, as the most promising model of sea clutter which enables realistic simulation of sea clutter, fits the data. The clutter from a single range cell was fitted to the theoretical K distribution PDF and shows a good fit. Thus leading to the conclusion that the K distribution clutter model can be used in the simulation of sea clutter and in analysing NetRad data.

Doppler spectrum of sea clutter obtained from a single range cell as plotted in Figure 5.6 shows the temporal variation of the clutter with Doppler frequency. The Doppler spectrum had positive frequency which is as expected as the sea waves moved towards the radar. The Doppler spectra as seen from NetRad has temporal features and as such may be reproduce with appropriate methods.

In an attempt to simulate temporal properties of sea clutter, Watt's [15] method was explored and implemented**.** Implementation was done as outlined in Section 3.3. This implementation as available in the program code in Appendix A did not yield promising result as the resulting Doppler spectrum did not have noticeable temporal properties as that from the radar data. A reason for this discrepancy might be in the generation of correlated gamma random samples with the ACF that matches the data set. Also from the Doppler spectra plots from data collected in earlier trials of the NetRad do not fully compare with plots obtained here. Although the methodology applied were similar, the discrepancy can be due to malfunctioning of the radar or some interference.

6.3 Further work

Further work will be to investigate further the simulation of temporal correlation of sea clutter. That is the generation of time varying spectra as can be observed from the NetRad data set. To expand Watts method [15] to allow for its application NetRad data set or explore other means to simulate the time varying Doppler spectra to be compared to that obtained from the NetRad data set.

Another area to be further investigated in this area of research is to consider trying more statistical test other than the K-S to test the validity of the results and to ensure that the generated K distribution

clutter indeed arises from the K distribution PDF.

And lastly to extend this monostatic sea clutter simulations to muiltistatic and in turn be able to compare results obtained with the muiltistaic sea clutter data from NetRad

Appendix A

Matlab toolbox description

This section describe the Matlab® toolbox for the generation of sea clutter.

To run the simulator to generate K distributed random variates, the following steps should be followed.

- First, determine what value of shape parameter to simulate. This is done by putting in the different inputs required into shape.m file. These inputs includes the sea state, the radar illumination area, the polarisation dependent parameter and the swell direction. Shape.m function uses Equation 2.7 to generate the K distribution shape parameter. Figure A.1 shows the M file extract from Matlab. This code will give the gamma distribution shape parameter.

- Next is to determine the radar parameters as well as environmental conditions. After this is done, one determines the clutter reflectivity from an illuminated patch of the sea. This is done by using the radar equation and σ^0 calculated from the GIT model presented in section 2.4.4 (see figure A.2 for code) to determine the scale parameter as explained in Chapter 4.

- Thereafter, load both the scale and shape parameter value into main.m. This main function [30] uses these value to compute the correlated K distributed variates. The main file and supporting functions are shown in figure A.3.

- The simulator produces correlated K distributed random variates with prescribe correlation function. Refere to Appendix C for Figures showing the normalised autocorrelation function as transformed via a gamma MNLT as a function of the shape parameter and the mapping between the input and output correlation functions.

- For coherent sea clutter analysis, processing was carried out on the raw data taken from the NetRad experimental radar system. This are stored in .mat format with an accompanying M file containing parameters of the trail.

```
% M file to calculate the gamma shape parameter given radar parameters and
% enviromental conditions
% Part of the Matlab Sea clutter simulator Toolbox by Titus Oyedokun
% Please acknowledge use of this toolbox in any publication or software.
% This header must be retained in any derivative work

% Ac =  alpha * rho * azumth_angle *sec(grazing angle)
% request for inputs... alpha, rho, azumth angle and grazing angle.
% azumptions a rectangle pulse ( chirp) a gaussian azimuth beam shape with
% azimuth angle defined to be the one-way 3 dB beamwidth. Thus set alpha to
% 0.753 ref

% [1] K D Ward and R J A Tough and S Watt, Sea Clutter: Scattering, the K distribution and Radar Performance
%(The Institution of Engineering and Technology, 2006).

Grazing_angle = input('enter grazing angle in degree: ')
Bandwidth = input('enter radar pulse bandwidth MHz: ')
antennaAZB = input('enter antenna azimuth beamwidth in degree: ')
slantR = input('enter slant range in meters : ')
heightH = input('enter height of radar above sea level in  meters : ')

c = 3e8; % speed of light
alpha = 0.753;
rho = c/(2*Bandwidth); % range resolution dependent on the radar pulse bandwidth
Ac = alpha*rho*antennaAZB*slantR*sec(Grazing_angle)

%using Wards et al. [empirical formula to calculate the shape parameter
kpol = 1.39 % for VV and 2.09 for HH
thetaS = 30 % aspect angle wrt the swell directions ( degree)
vlong =(2/3)*log10(Grazing_angle) + (5/8)*log10(Ac) - kpol - cos(2*thetaS)/3;

v = exp(vlong) % extract v, the shape parameter
```

Figure A.1: Code for calculating the K distribution shape parameter [2]

```
Seastate = input('Enter sea state : ')
Grazing_angle = input('enter grazing angle in degree: ')
radarwavelength = input('Enter radar wavelength in meters : ')
winddirection = input('Enter wind direction : ')

Mean_clutter = input('Please enter 1 for vertical or 2 for holizontal polirsation : ');
lambda = radarwavelength;
U = 3.16*Seastate^0.8; %windvelocity
waveheight = 0.00452*U^2.5; %Wave height
RoughPar = (14.4*lambda + 5.5)*(Grazing_angle*waveheight)/lambda; % Roughness parameter
Winddepen = exp(0.2*cos(winddirection)*(1-2.8*Grazing_angle)*(lambda+ 0.015)^-0.4); %wind dependence
SeaVara = (1.94*U)/(1+(U/15.4))^1.1/(lambda + 0.015)^0.4; % Variation on sea state

% Mean clutter reflectivity for vartical and holizontal polisation

SigmaO = 65.91 + 10*log10(lambda*Grazing_angle^0.4*SeaVara*Winddepen*RoughPar);
if Mean_clutter == 1
    SigmaO = 65.91 + 10*log10(lambda*Grazing_angle^0.4*SeaVara*Winddepen*RoughPar)
else
   SigmaO = SigmaO -1.05*log(waveheight+0.015) + 1.09*log(lambda) + 1.27*log(Grazing_angle + 0.0001) + 9.7
end

%Calculate the Sigma ( Clutter Reflectivity)
%Sigma = mean reflectivity * the illuminated area

Antenna_beam_width = input('Antenna beam-width : ')
range_resolution = input ('range resolution : ' )
range = input('range of the radar : ')
A = Antenna_beam_width*range_resolution*range* sec(Grazing_angle); % Illuminated area of clutter Ac

Clutter_reflectivity = SigmaO* A;
```

Figure A.2: Code for calculating the Clutter reflectivity for an illuminated area. [2]

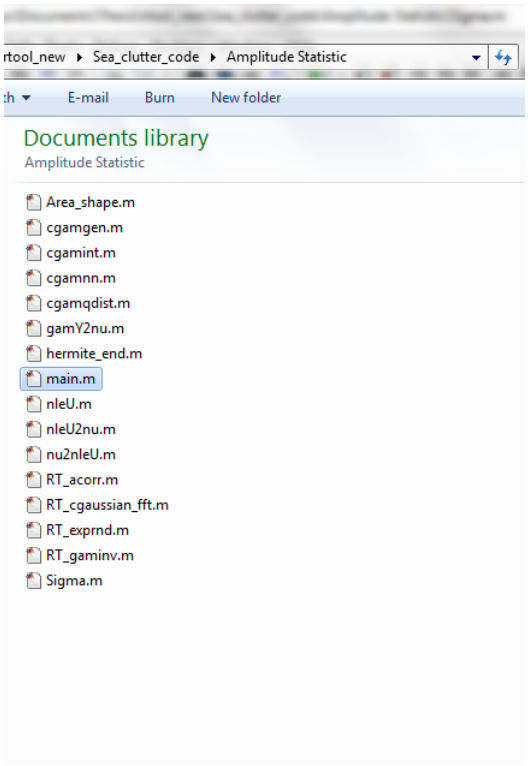

Figure A.3: Folder containing functions for the simulator.

- Using NetradExtract.m from the folder as seen in Figure A.4, the file is read and matched filtered.
- Spectra_analysis.m calculates and gives the plots as seen in section 5.3.

A.0.1 Test Case

Figures A.5 and A.6 shows the result for different shape parameter. This agrees with literature as higher value of shape parameter means less clutter amplitude while the lower the shape parameter the higher the clutter is in amplitude.

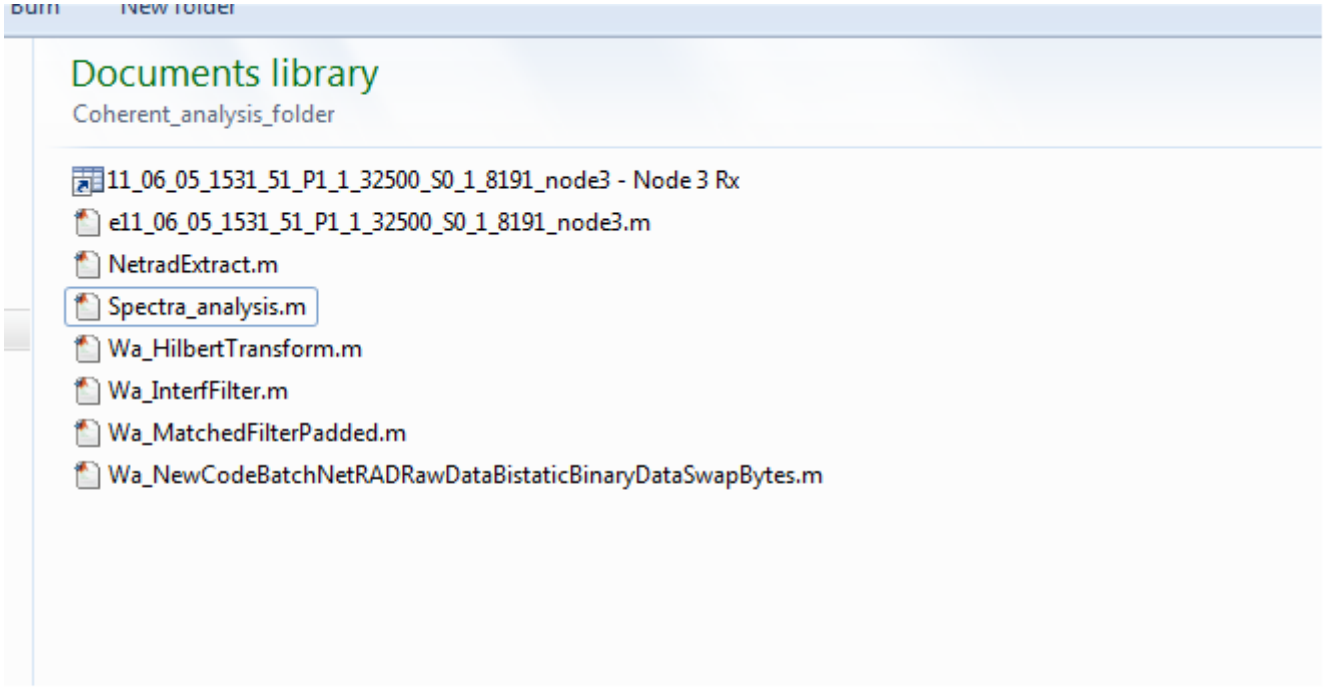

Figure A.4: Folder containing functions for the spectra analysis from NetRad data set

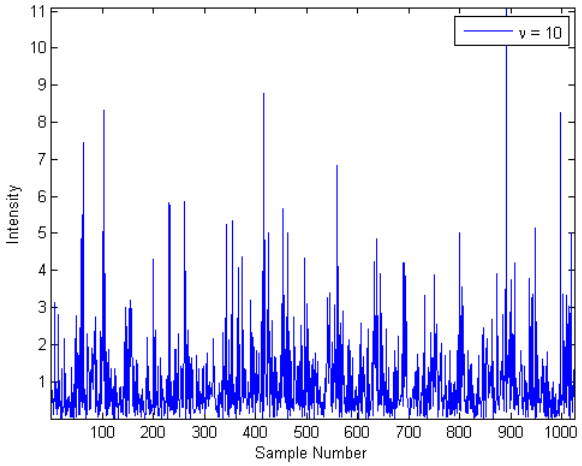

Figure A.5: Correlated K distributed random variate with shape parameter 10 and scale parameter set to Unity

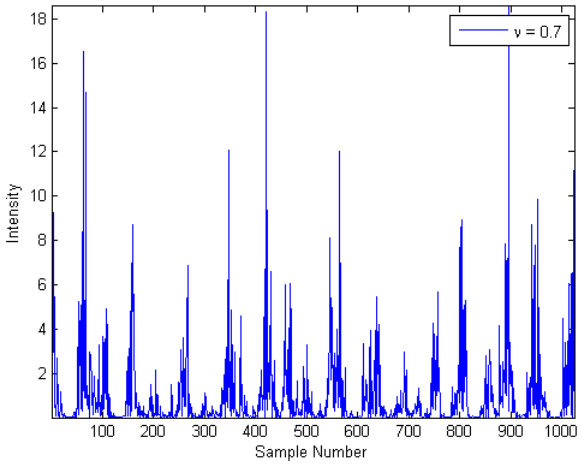

Figure A.6: Correlated K distributed random variate with shape parameter 0.7 and scale parameter set to Unity

Appendix B

GIT mean sea clutter reflectivity model

The Georgia Institute of Technology (GIT) model for the mean sea clutter reflectivity covers a range of radar frequencies from 1 to 10 GHz and is based on an underlying multipath model as well as other more general treads observed in experimental data sets. This model is as follows [2]
The wind velocity, U, is derived from the sea state, s

$$U = 3.16s^{0.8}$$

The average wave height, h_{av}, is given by

$$h_{av} = 0.00452U^{2.5}$$

A roughness parameter is defined as

$$\sigma_\phi = (14.4\lambda + 5.5)\frac{\phi_{gr}h_{av}}{\lambda}$$

where λ is the radar wavelength and $\phi_{gr}$is the grazing angle. This acts as an interference factor

$$A_i = \frac{\sigma_\phi^4}{1+\sigma_\phi^4}$$

The wind dependence is related to the grazing angle and the wind direction through

$$A_i = \exp(0.2\cos(\theta_w)(1-2.8\phi_{gr})(\lambda+0.015)^{-0.4})$$

where $\theta_w$is the wind direction relative to the radar look direction.
The variation on sea state is given by

$$A_w = (\frac{1.94U}{1+(U/15.4)})^{1.1/(\lambda+0.015)^{0.4}}$$

There the mean clutter reflectivity for different polarisation is given by

$$\sigma^0_{HH} = 65.91 + 10log_{10}(\lambda \phi^{0.4}_{gr} A_i A_u A_w)$$

$$\sigma^0_{vv} = \sigma^0_{HH} - 1.05log_e(h_{av} + 0.015) + 1.09log_e(\lambda) + 1.27log_e(\phi_{gr} + 0.0001) + 9.7$$

Appendix C

MNLT method

Figure C.1 shows the polynomial fit for the inversion to directly generate a Gamma with the desired correlation. The inverse of the modification to Rg is calculated using a 4th order polynomial fit.

Figure C.2 shows how the input normalised autocorrelation function is transformed via a gamma MNLT as a function of the shape parameter.

Figure C.3 is another example of simulated correlated K distributed random variates with shape parameter 5 and unit mean.

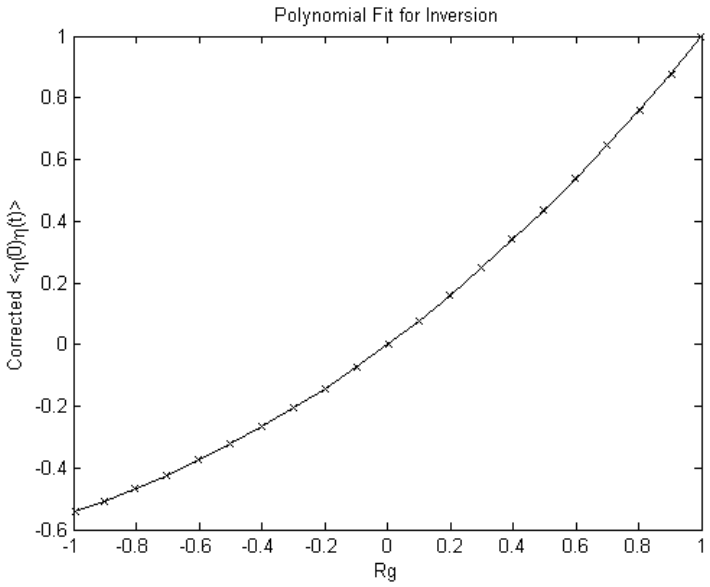

Figure C.1: Mapping between the input and output correlation functions

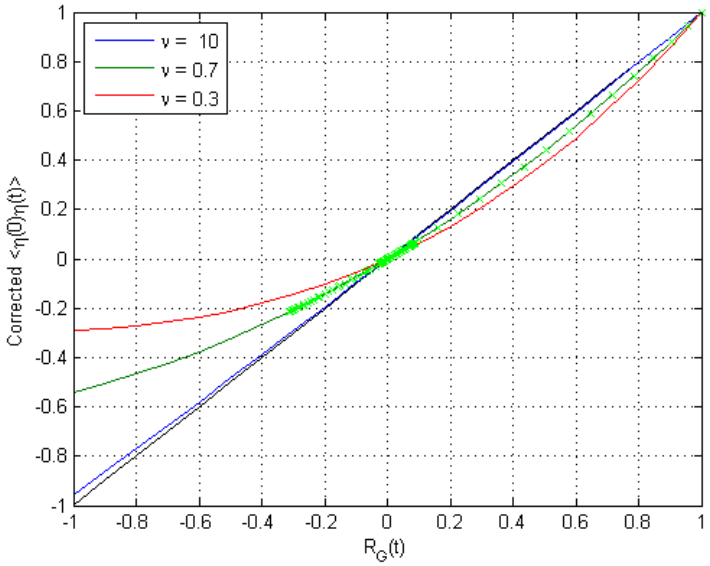

Figure C.2: The normalised ACF value transformation via a gamma MNLT as a function of shape parameter *v*

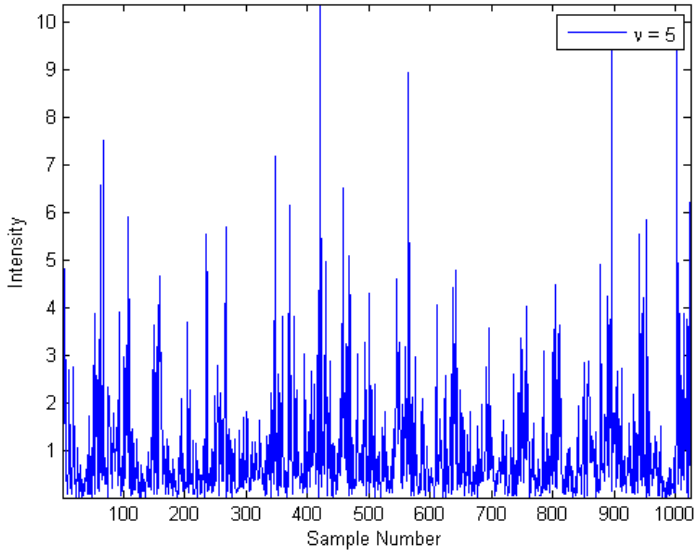

Figure C.3: Correlated K of a shape parameter 5, unit mean.

Appendix D

Doppler spectrum from NetRad

The NetRad results shown in Appendix D are the outcome of the Doppler processing of different recordings obtained using NetRad. These were obtained on different days with varying weather and environmental conditions.

Figures D.1 and D.2 shows the time history and the Doppler spectrum of the clutter from a single range cell taken from "11_06_05_1108_39_P1_1_130000_S0_1_2047_node3 - Node 3 Rx.mat" data set. Figures D.3 and D.4 are taken from "11_06_07_1129_51_P1_1_32500_S0_1_8191_node3 - Node 3 Rx.mat"

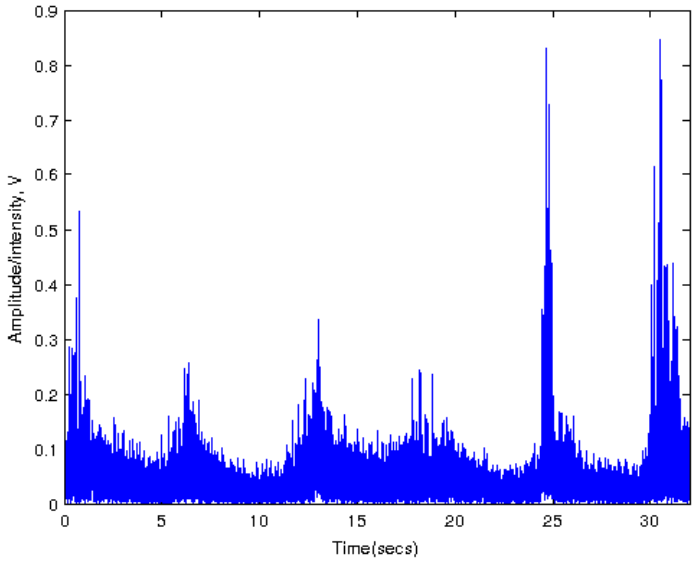

Figure D.1: Time history of the clutter amplitude from a single range cell

The raw data was the processed over a burst of L = 64 samples with a fast Fourier transform (FFT) and using a -55 dB Dolph-Chebyshev weighting function in the time domain. Figures D.2 and D.4 shows the power spectra density of the data for 500 successive spectra corresponding to 32 seconds. As seen, the spectrum width varies with time, with Doppler excursions as seen around 10

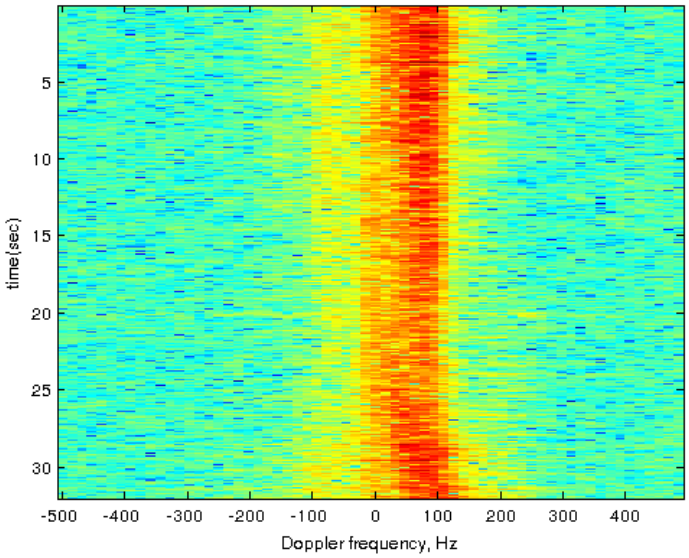

Figure D.2: Doppler spectra (dB) from a single range cell , f_r = 1kHz, FFT length l = 64, -55 dB Doplh-Chebyshev window

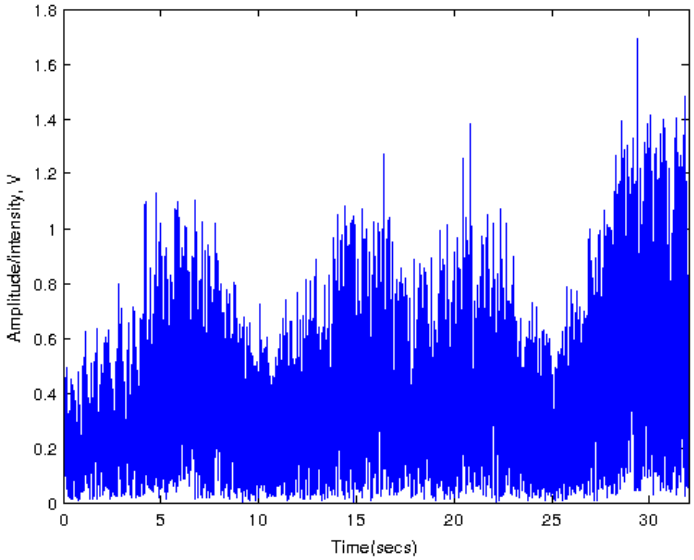

Figure D.3: Time history of the clutter amplitude from a single range cell

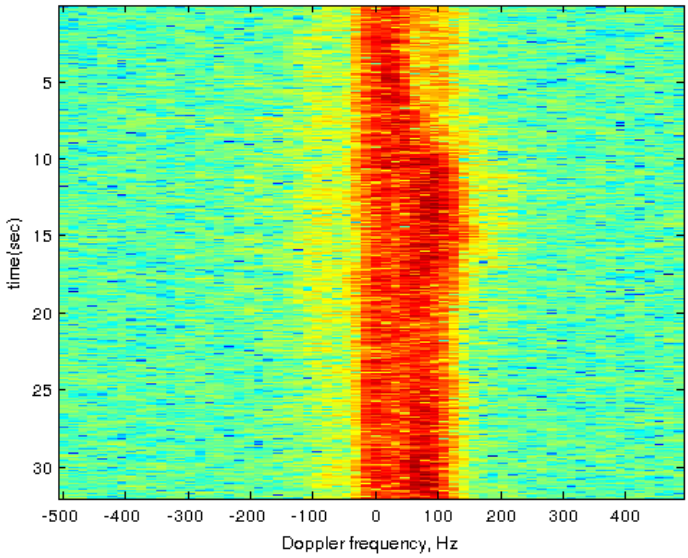

Figure D.4: Doppler spectra (dB) from a single range cell f_r = 1kHz, FFT length l = 64, -55 dB Doplh-Chebyshev window

seconds which might be as a result of local wind gusting. Also noted is the asymmetric nature of the spectrum. Overall, the spectrum looks well-behaved, with a non-zero mean Doppler shift which appears to vary with time.

However, also observed from Figures D.2 and D.4 is a strong DC line. Figure D.4 has a very high Doppler frequency content appearing at 100 Hz. Comparing this spectrum to early NetRad recording as published by Inggs et al [4] there are some observed differences in the Doppler spectra obtained. This is probably due to interference during measurements.

Bibliography

[1] R. J. A. Tough and K. D. Ward, "The correlation properties of gamma and other non-gaussian processes generated by memoryless nonlinear transformatio," *J. Phys. D; Appl Phys*, vol. 32, pp. 3075–3084, 1999.

[2] K. D. Ward, R. J. A. Tough, and S. Watts, *Sea Clutter: Scattering, the K distribution and Radar Performance*. The Institution of Engineering and Technology, 2006.

[3] A. Farina, F. Gini, M. Greco, and L. Verrazzani, "High resolution sea clutter data: statistical analysis of recorded live data," *Radar, Sonar and Navigation, IEE Proceedings* -, vol. 144, pp. 121 –130, June 1997.

[4] M. Inggs, G. Inggs, S. Sandenbergh, W. Al-Ashwal, K. Woodbridge, and H. Griffiths, "Multistatic networked radar for sea clutter measurements," in *Geoscience and Remote Sensing Symposium (IGARSS), 2011 IEEE International*, pp. 4449 –4452, July 2011.

[5] E. F. Nathanson, J. P. Reilly, and N. M. Cohen, *Radar Design Principles- signal Processing and the environment*. Scitech Publishing Inc, 1999.

[6] K. Ward and S. Watts, "Use of sea clutter models in radar design and development," *Radar, Sonar Navigation, IET*, vol. 4, pp. 146 –157, April 2010.

[7] S. Watts, C. Baker, and K. Ward, "Maritime surveillance radar. ii. detection performance prediction in sea clutter," *Radar and Signal Processing, IEE Proceedings F*, vol. 137, pp. 63 –72, April 1990.

[8] M. Brooker, *The Design and Implementation of a Simulator for Multistatic Radar Systems*. Doctoral thesis, University of Cape Town - RRSG, June 2008.

[9] I. Antipov, "Simulation of sea clutter returns," *IET Radar Sonar Navigation*, vol. DSTO-TR-0679, pp. 146–157, June 1998.

[10] G. Davidson, "Simulation of coherent sea clutter," *Radar, Sonar Navigation, IET*, vol. 4, pp. 168 –177, April 2010.

[11] X. Li and X. Xu, "A statistical model for correlated k-distributed sea clutter," in *Image and Signal Processing, 2008. CISP '08. Congress on*, vol. 5, pp. 408 –412, May 2008.

[12] W. Szajnowski, "The generation of correlated weibull clutter for signal detection problems," *Aerospace and Electronic Systems, IEEE Transactions on*, vol. AES-13, pp. 536 –540, September. 1977.

[13] P. Peebles, "The generation of correlated log-normal clutter for radar simulations," *Aerospace and Electronic Systems, IEEE Transactions on*, vol. AES-7, pp. 1215 –1217, November. 1971.

[14] D. Yunhan, "Clutter spatial distribution and new approaches of parameter estimation for weibull and k distribution," tech. rep., DSTO Electronic and Surveillance Research Laboratory, April 2004.

[15] S. Watts, "A new method for the simulation of coherent sea clutter," in *Radar Conference (RADAR), 2011 IEEE*, pp. 052 –057, May 2011.

[16] H. Griffiths, W. Al-Ashwal, K. Ward, R. Tough, C. Baker, and K. Woodbridge, "Measurement and modelling of bistatic radar sea clutter," *Radar, Sonar Navigation, IET*, vol. 4, pp. 280 –292, April 2010.

[17] K. Ward, C. Baker, and S. Watts, "Maritime surveillance radar. i. radar scattering from the ocean surface," *Radar and Signal Processing, IEE Proceedings F*, vol. 137, pp. 51 –62, April 1990.

[18] A. Irina, "Analysis of sea clutter data," *DSTO Electronic and Surveillance Research laboratory*, vol. DSTO-TR-0647, June 1998.

[19] C. Baker, "K-distributed coherent sea clutter," *Radar and Signal Processing, IEE Proceedings F*, vol. 138, pp. 89 –92, Apr 1991.

[20] A. Farina, F. Gini, M. Greco, and L. Verrazzani, "Analysis of sea clutter radar data," in *Radar, 1996. Proceedings., CIE International Conference of*, pp. 115 –118, October 1996.

[21] Y. Dong, "Clutter spatial distribution and new approaches of parameter estimation for weibull and k- distribution," in *DSTO systems Sciences Laboratory, Edinburgh South Australia*, April 2004.

[22] K. Ward, R. Tough, and P. Shepherd, "Modelling sea clutter: correlation, resolution and non-gaussian statistics," in *Radar 97 (Conf. Publ. No. 449)*, pp. 95 –99, October 1997.

[23] S. Watts, K. Ward, and R. Tough, "Modelling the shape parameter of sea clutter," in *IEE Proceedings-Radar, Sonar Navigation*, 2009.

[24] A. Parthiban, J. Madhavan, P. Radhakrishna, D. Savitha, and L. Kumar, "Modeling and simulation of radar sea clutter using k-distribution," in *Signal Processing and Communications, 2004. SPCOM '04. 2004 International Conference on*, pp. 368 – 372, December. 2004.

[25] S. Watts, K. Ward, and R. Tough, "Modelling the shape parameter of sea clutter," in *Radar Conference - Surveillance for a Safer World, 2009. RADAR. International*, pp. 1 –6, October. 2009.

[26] M. Ritchie, K. Woodbridge, and A. Stove, "Analysis of sea clutter distribution variation with doppler using the compound k-distribution," in *Radar Conference, 2010 IEEE*, pp. 495 –499, May 2010.

[27] A. Leon-Garcia, *Probability and Random Processes for Electrical Engineering*. Addision-Wesley publishing company, 1989.

[28] B. D. Ripley, *Stochastic Simulation*. John Wiley & Sons, 1987.

[29] J. E. Gentle, *Random Number Generation and Monte carlo Methods*. Springer, second ed., 2003.

[30] G. Davidson, "www.radarworks.com."

[31] A. Papoulis, *Probability, Random variables and stochastic processes*. McGraw-Hill Inc, second edition ed., 1991.

[32] T. Oyedokun and M. Inggs, "Design and evaluation of a sea clutter simulator," in *Geoscience and Remote Sensing Symposium (IGARSS), 2011 IEEE International*, pp. 2089 –2092, July 2011.

[33] T. Derham, S. Doughty, K. Woodbridge, and C. Baker, "Design and evaluation of a low-cost multistatic netted radar system," *Radar, Sonar Navigation, IET*, vol. 1, pp. 362 –368, October 2007.

[34] T. Derham, K. Woodbridge, H. Griffiths, and C. Baker, "The design and development of an experimental netted radar system," in *Radar Conference, 2003. Proceedings of the International*, pp. 293 – 298, September. 2003.

[35] J. Sandenbergh and M. Inggs, "A common view gpsdo to synchronize netted radar," in *Radar Systems, 2007 IET International Conference on*, pp. 1 –5, October. 2007.

[36] A. Hume and C. Baker, "Netted radar sensing," in *Radar Conference, 2001. Proceedings of the 2001 IEEE*, pp. 23 –26, 2001.

Declaration

I declare that this dissertation is my own, unaided work. It is being submitted for the degree of Master of Science in Engineering in the University of Cape Town. It has not been submitted before for any degree or examination in any other university.

Signature of Author . . . . . Signed by candidate Signature Removed . . . . . .

Cape Town

14 May 2012

Dissertation Topic: Sea Clutter Simulation

Report on Corrections

Signed by candidate

Titus Oluwale Oyedokun (OYDTIT001) Signature Signature Removed

Date: 14/05/2012

Supervisor: Prof Michael Inggs

1 Introduction

This report describes detailed response to the examiners' report on the dissertation entitled "Sea clutter simulation submitted by the author to the faculty of Engineering and Built environment at the University of Cape Town in partial fulfillment of the requirements for the Degree of Masters of Science in Engineering. Three examiners report has been received by the author. Here, each examiner's comments will be addressed giving detailed responses. In this document, the examiners' reports are referred to as Examiner's report A, Examiners report B and Examiners report C.

Corrections given by Examiner A largely relate to typographical and grammatical errors and also to give more clarification on some comments in the dissertation where necessary. These changes have been applied throughout the dissertation.

Examiner's Report B also relates mainly to typographical and grammatical errors. The applicable changes have been applied throughout the dissertation.

Examiner's Report C gave four major technical suggestions to this dissertation and also various minor corrections relating to typographical and grammatical errors. The four major technical suggestions have also been addressed below.

The following are a list of the examiner's report comments and author's responses.

2 Examiner's Report A

Item Number: 1

Document reference: Page xi

Examiners: The table of symbols is incomplete.

Response: This table has been updated. The following were added to the list of symbols.

σ^0	---	Clutter reflectivity
β	---	Weibull scale parameter
α	---	Weibull shape parameter
G	---	Antenna gain
L	---	propagation and other losses

Item number: 2

Document reference: Throughout dissertation.

Examiner: Various typographical and grammatical errors.

Response: Typographical and grammatical corrections have been implemented where necessary as pointed out by the examiners throughout the dissertation.

Item number: 3

Document reference: Page 1, Para 3

Examiner: Explain why the compound representation of the clutter processes is needed.

Response: This has been incorporated into the thesis with the following explanation as to why the compound representation of the clutter process is needed which was not previously explained.

When sea clutter is measured over a relatively short time interval of about a second, the sea clutter returns shows a negative exponential distribution often referred to as Gaussian speckle. This clutter returns decorrelates completely within the interval of observation. However, as the observation time increases, the statistics of the observed clutter varies from that of just the Gaussian shape but can now be approximated by the gamma distribution. Thus the Gaussian speckle and its gamma distributed randomly varying local power are brought together in the compound K model of sea clutter. The correlation properties of the more slowly varying gamma component of the clutter are the one that affects the radar performance. Thus the need of the compound representation of the clutter processes [1].

Item number: 4

Document reference: page 10, Figure 24.

Examiners: Explain the time-series data and how they are generated.

Response: The paragraph below has been included giving detailed explanation on how this time series data was obtained.

The time series data was generated from the Weibull PDF. Implementing the mathematical description of the Density function in Matlab code, Weibull random clutter was generated. The Weibull shape parameter and scale parameter was varied to give the Figure 2.4 as shown in the dissertation. This also applies to the examiners question about Figure 2.5. The lognormal distribution PDF was plotted for different mean and variance. Figure 2.6 shows the K distribution PDF also plotted for various shape and scale parameters. In each case, the time-series data was generated using the inbuilt random number generator functions in Matlab.

Item Number: 5

Document reference: Page 18, Section 3.2.1.

Examiner: The description is rather muddled.

Response: In section 3.2.1 it was mentioned that the MNLT provided a map from zero mean correlated Gaussian process to a correlated Gamma process with the required correlation. This which was pointed out by the examiner is not necessarily the case. The MNLT is given by Equation (3.1) in the dissertation. To generate correlated gamma process, a correlated Gaussian process of zero mean and unit variance should be taken as the starting point. This is then mapped onto a gamma process by the memoryless nonlinear transform (MNLT) generated by the solution of Equation (3.1).

Item Number 6

Document reference: Page 19 Section 3.2.2

Examiner: Your description completely omits the most important step in this process – How to determine the correct correlation of the Gaussian samples before applying the MNLT**.**

Response: A new Section has been added just after Section 3.2.1. This section titled the generation of correlated Gaussian random samples (Section 3.2.2) explains how the correct correlation of the Gaussian samples is determined. With the aid of a flow chat as now seen in Figure 3.1 in the dissertation and also here in the Figure 1 below, the processes has been explained. Here, in this dissertation, the Fourier synthesis method of random processes has been applied in the generation of correlated Gaussian random samples with prescribed correlation function [3]. Implementation of this process is available in program code. And a description of the simulation package can be found in Appendix A.

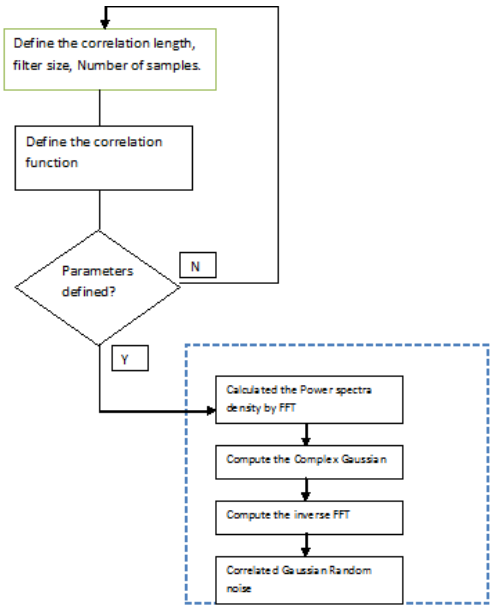

Figure 1 Flow chart showing the generation of correlated Gaussian random variates

---

Item Number: 7

Document reference: page 31, Figure 4.7

Examiner: How many tests were done to produce Figure 4.7?

Response: The result shown in Figure 4.7 was carried for a set of data obtained from the simulator for a given K distribution shape parameter. More tests have been carried out and the outcome is explained in Examiner's B report response below.

Item Number: 8

Document reference: Page 40, Summary

Examiner: The discussion and conclusion on the fit to a Gaussian spectrum shape needs to be reviewed.

Response: As the examiner correctly points out that on page 32 Para 2, the spectra shown in Figure 5.6 does not have a Gaussian shape as such this section is reviewed.

In page 40, the chapter summary, it was mentioned that from Figure 5.7 the average spectrum over a group of 10 successive spectra fits the Gaussian model thus assuming a Gaussian model for the Doppler spectrum. This assumption is not readily visible from the plots provided in Figure 5.7 and as

such further work will have to be carried out to establish such relationships. Figures 5.6 and 5.7 have been removed from the dissertation.

The shape of the power spectral densities as they evolve over time will need to be reexamined by further analysis. From the batch of NetRad result processed in this dissertation, some artifacts have been observed in the Doppler spectra. Other dataset from various trials will have to be analysed to be able to draw up a comparison of the power spectral densities to a Gaussian shape spectrum.

Item number: 9

Document Reference: Appendix C:

Examiner: The material here is not discussed or referenced in this dissertation.

Response: Most of the figures present in Appendix C have to do with the generation of correlated K distributed random variates from a given correlated Gaussian samples by using the method of Ward and Tough [1].

And enhanced explanation pointing to this Appendix has been added to Section 3.2. Figures C1 and C2 shown in appendix C includes the mapping between the input and output correlation functions and the normalized ACF value transformation via a gamma MNLT as a function of shape parameter v.

Item Number: 10

Document reference: Page 53 et seq

Examiner: Comment on NetRad results shown in Appendix D.

Response: Comments have now been added to this appendix to explain the result obtained from the NetRad trials which are presented in Appendix D.

The NetRad results shown in Appendix D are the outcome of the Doppler processing of different recordings obtained using NetRad. These were obtained on different days with varying weather and environmental conditions.

Figure D.1 and D.3 shows the time history of the observed clutter from a single range gate. This was obtained by calculating the power spectra density of the data for 500 successive spectra corresponding to 32 seconds while Figure D.2 and D.4 are the Doppler spectra (dB) plots from a single range cell of FFT length l =64, -55 dB Doplh-Chebyshev window applied to the data.

Item Number: 11

Document reference: Page 56 et seq. Bibliography

Examiner: Some information missing in the reference/Bibliography

Response: The Bibliography has been corrected to meet the required standard.

- All listed references have now been made referenced to in the dissertation
- The DSTO report number has been included in references [14], [16], and [19]

4 Examiner's Report B

Examiner: typographical and grammatical errors.

Response: corrections have been done.

5 Examiner's Report C

Technical suggestion: The MNLT algorithm has been used extensively in the work. Hence, a detailed presentation of the MNLT algorithm is needed (Preferably before Section 3.3)

Response: The MNLT algorithm has been explained through Section 3.2.1 to 3.2.2. This presented the method used to generate correlated gamma distributed random numbers with prescribed correlation function.

The intention here was to present this method first by giving a brief description of the MNLT method as developed by Ward and Tough [1]. However, a new section (Section 3.2.2) has been added to Chapter 3 to enhance the explanation on the generation of correlated K distributed random varites. This Section explains the process taken in the generation of correlated Gaussian random samples before applying the MNLT process.

Technical suggestion: The student has used Kolmogorov-Smirnov (K-S) test to validate his results (Page 31). However, this analysis needs a more rigorous treatment. Given that this is the only place the proposed algorithm is tested, the student should expand the section on it, do the K-S analysis for more data and present the trends. He can also consider trying one more metric to test the validity of the results.

Response: Previously as seen in Figure 4.7 in the dissertation and shown here in the Figure 2 below, the test was carried out on a given set of data for a particular K distribution shape parameter. Here the test passed the Null hypothesis which was to determine if the generated correlated K distributed random variates indeed arise from the K distribution. As it was observed in the figure and noted down in the dissertation it did pass.

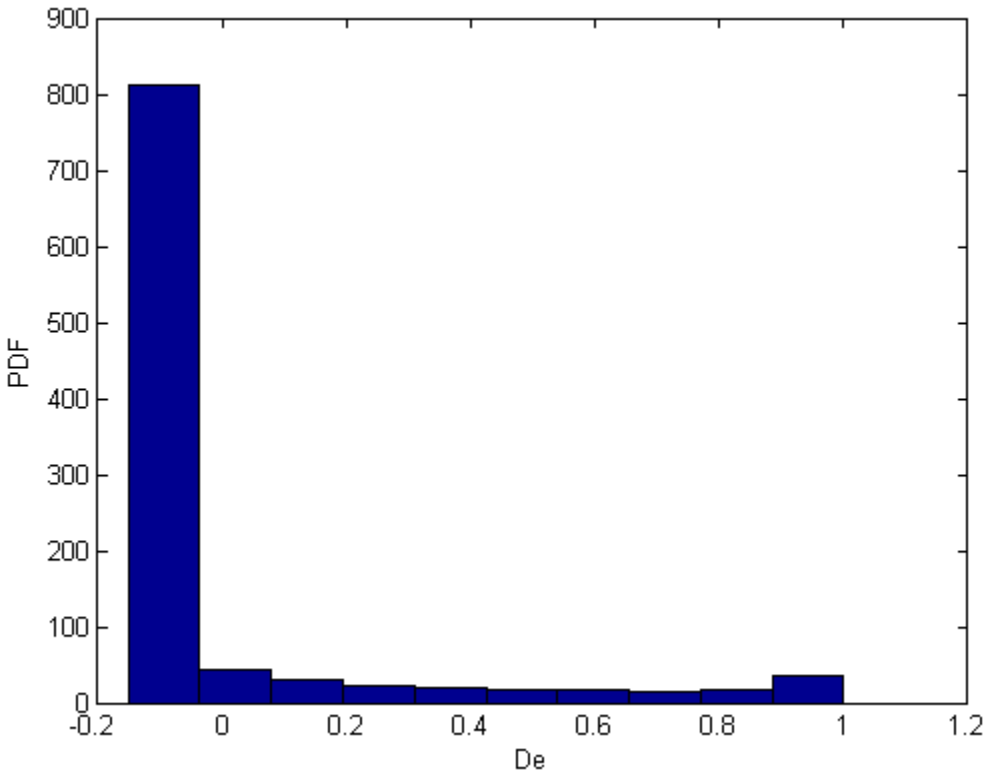

Figure 2 The probability density function for D_{e} values of the Kolmogorov-Sminov test

In response to the examiners' comments about analysing more data using this test, this has been done and the results are presented in the dissertation in Section 4.3.3. More analysis has been carried out for different values of the K distribution shape parameter. The results obtained shows that the K-S test passed only for smaller values of the shape parameter.

The simulation outcomes are tested using the K-S test. By varying the sea clutter shape parameter and obtaining different outcomes more analysis has been carried out. Figure 4.8 to 4.11 now in the dissertation shows the K-S test of more data from the simulator. This presents the test done for different values of the shape parameter. Table 4.1 tabulates the results for a confidence level of 5%. It can be noted that only data obtained for small values of the shape parameter passed the null hypothesis test. Table 4.1 in the dissertation and as shown here (in Table 1) tabulates the results obtained.

Table 1 Table showing results obtained from the K-S test of different data corresponding to different K distribution shape parameter

Shape parameter	h	k
v = 0.7	0	0.1058
v = 5	1	0.8662
v = 10	1	0.9603
v = 0.8	0	0.1342

The h indicates the result of the null hypothesis. h = 1 if the test fails the null hypothesis with a 5% significance level and h = 0 otherwise. k gives the test statistic of the maximum difference between the two CDF curves.

The Figures 3 to 7 shows the Empirical CDF versus the CDF from the simulated Clutter.

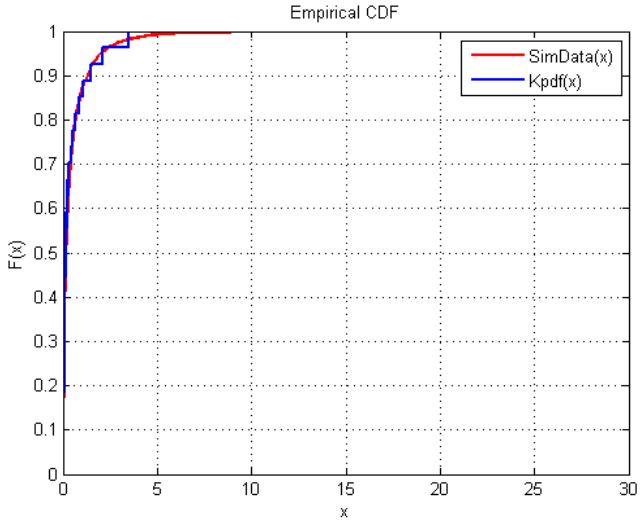

Figure 3 The K-S test for K distribution shape parameter v = 0.8

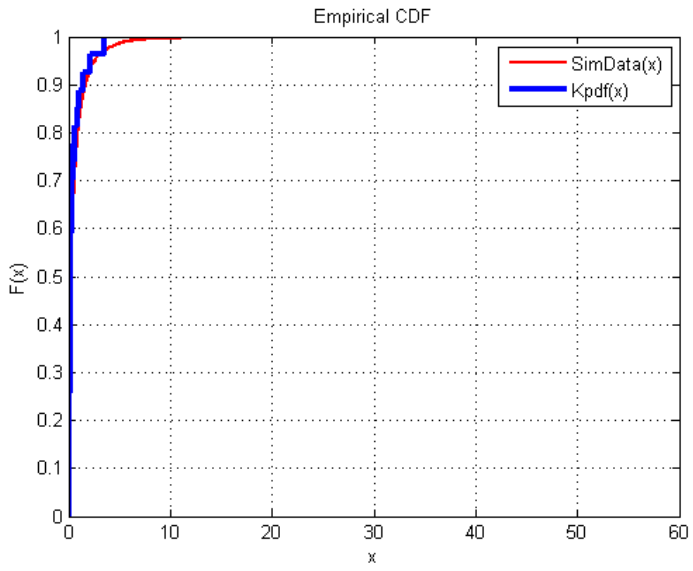

Figure 4 The K-S test for K distribution shape parameter v = 0.8

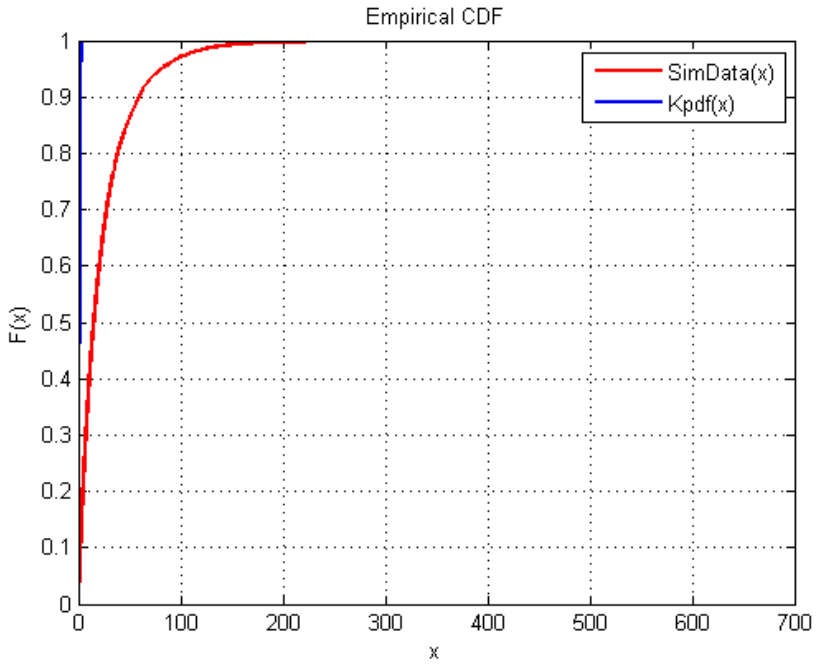

Figure 5 The K-S test for K distribution shape parameter v = 5

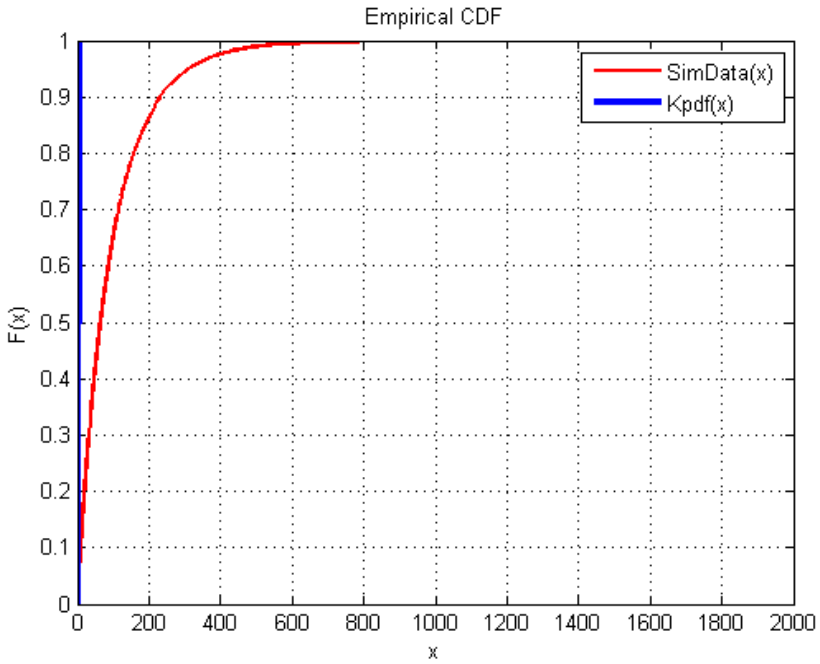

Figure 6 The K-S test for K distribution shape parameter v = 10

This trend shows that for the simulator output having smaller value of shape parameter, i.e very spiky clutter, and the results passes the K-S test while for larger values of the shape parameter, the test fails the null hypothesis. In such cases, further analysis would have to be carried out. Further work will be to try other statistical test to test the validity of the results.

Technical suggestion: In Section 3.3, the thesis presents the major contribution of the work, viz the algorithm to simulate coherent sea clutter. This section needs to be expanded substantially and the algorithms should also be presented as a flow chart and as a pseudo-code

Response: Section 3.3 presented a step by step description of the processes taken to simulate coherent sea clutter using the recent method as developed by Watts [2]. The proposed method is thus present here step by step**.** A flow chat (shown in Figure 3.5) has been added to this section. This flow chart presents the various steps followed to simulates sea clutter Doppler spectra having temporal properties as those observed from the real sea clutter data. The flow chat is given below (Figure 7).

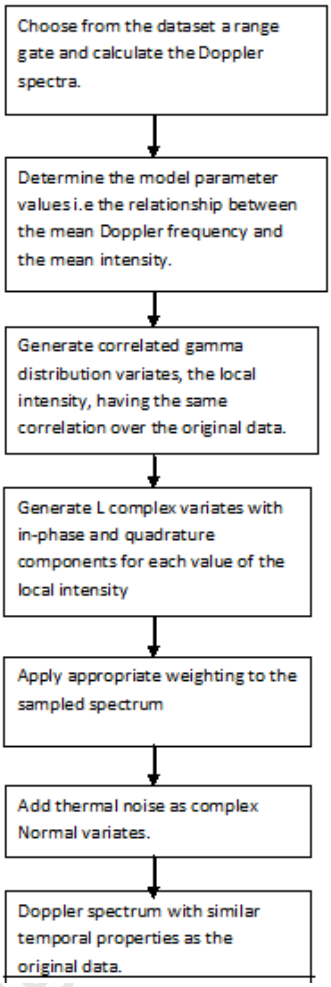

Figure 7 Flow diagram showing the algorithm for the simulation of sea clutter Doppler spectra

---

Technical suggestion: In Chapter 5, the thesis discusses the comparison of the simulated data with field-collected data. First of all why has the comparison with simple monostatic case not discussed. Secondly, the data collected was multi-static and hence expects to have drastically different clutter statistics. The simulation algorithms have all been discussed for a monostatic configuration. How can monostatic simulated clutter be compared to multistatic clutter? Lastly, the results in this Chapter 9 as shown in Figures 5.3-5.8) need to be explained. There is hardly any explanation of the results.

Response: The simulation of monostatic sea clutter in this dissertation deals with the generation of K distributed random variates having a predefined shape parameter. NetRad, although a radar capable of muiltistatic radar measurements, also has the ability to record monostatic radar data.

Measurements taken for the data set used in this analysis was done at Scarborough cape Town. With the transmitter and receiver node 3 placed at Misty Cliff and the receiver node 1 and 2 placed

some distance apart. Only the monostatic data, that is, from receiver node 3 are considered in this project**.** This statement has now been added which was previously not mentioned to make clear in the introduction to Chapter 5 of the dissertation that all results used from the NetRad measurements are monostatic. The discussion below is to explain the comments given to Figures 5.3 to 5.6 in the dissertation.

Figures 5.6 in the dissertation (and Figure 8 in this correction report) show the Doppler spectra from a single range cell. The raw data was the processed over a burst of L = 64 samples with a fast Fourier transform (FFT) and using a -55 dB Dolph-Chebyshev weighting function in the time domain.

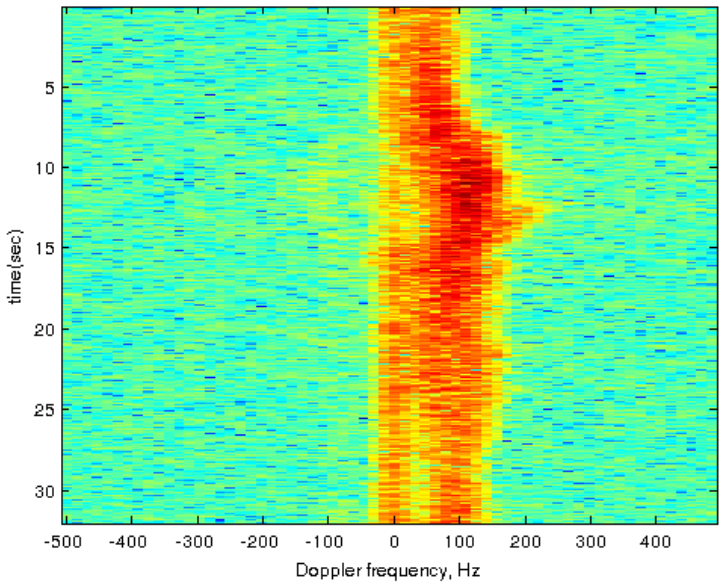

Figure 8 Doppler spectra (dB) from a single range cell;f_{r} = 1kHz, FFT length l = 64, -55 dB Doplh-Chebyshev window

As seen, the spectrum width in Figure 5.6 varies with time, with Doppler excursions as seen around 10 seconds which might be as a result of local wind gusting. Also noted is the asymmetric nature of the spectrum. However, also observed from Figures 5.6 there is a strong DC line and also has a very high Doppler frequency content appearing at 100 Hz. This is probably due to interference during measurements.

Figures 9 and Figure 10 (and Figure 5.4 and Figure 5.5 In the dissertation) shows a comparison of the amplitude distribution of the clutter to the proposed clutter model. The data from the range cell was fitted to Rayleigh, K distribution and the Weibull PDF distribution. As seen in Figure 9, the data set shows to fit the K distribution well more than the Rayleigh distribution. Furthermore, the moments up to the sixth order as seen in Figure 10 was computed and compared to the theoretical K, Rayleigh and Weibull moments shown in Figure 10. The data shows a good agreement with the K distribution.

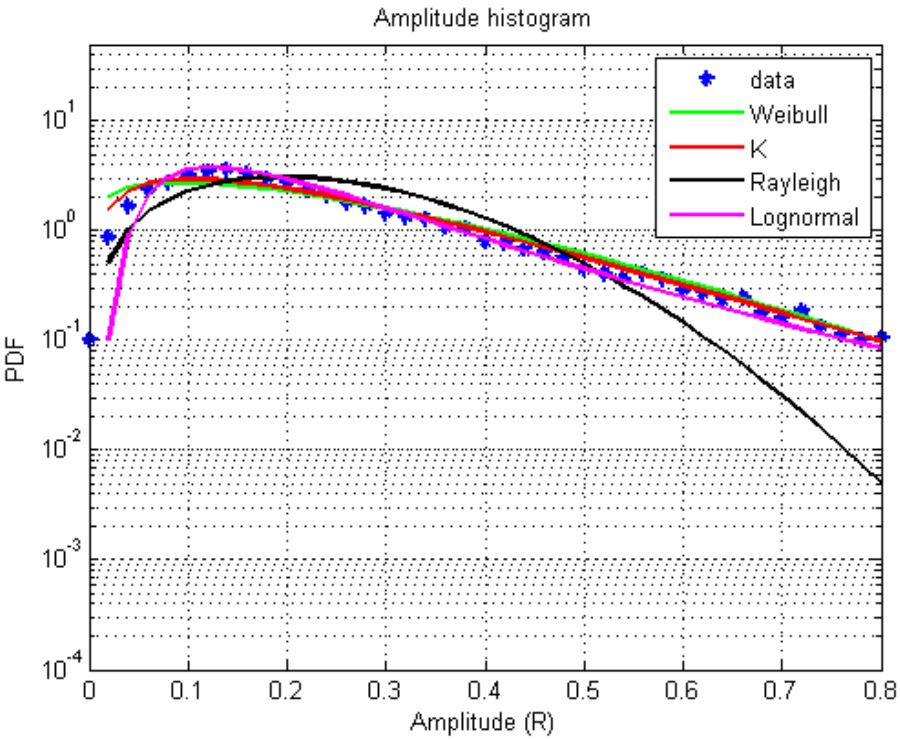

Figure 9 Amplitude histogram of the data fitted to different distributions

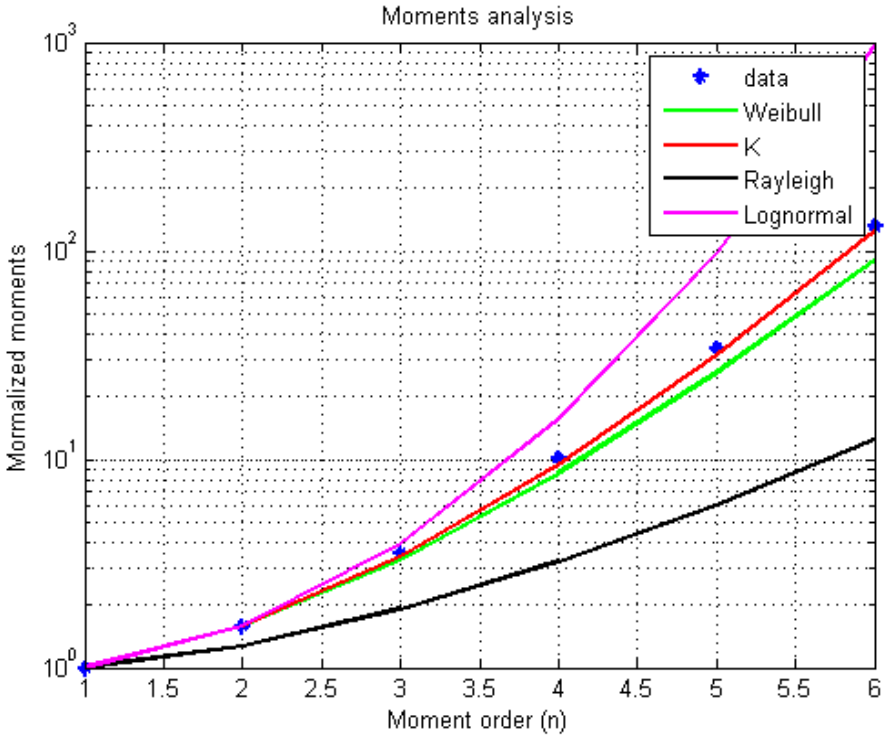

Figure 10 Normalised moment versus moment order

Reference

[1] R. J. A. Tough and K. D. Ward, “The correlation properties of gamma and other non-gaussian processes generated by memoryless nonlinear transformation,” J. Phys. D; Appl Phys, vol. 32, pp. 3075–3084, 1999.

[2] S. Watts, “A new method for the simulation of coherent sea clutter,” in Radar Conference (RADAR), 2011 IEEE, pp. 052 –057, May 2011.

[3] K. D. Ward, R. J. A. Tough, and S. Watt, Sea Clutter: Scattering, the K distribution and Radar Performance. The Institution of Engineering and Technology, 2006